Course 2024–2025 in Sustainable Finance
Lecture 9. Awareness of Climate Change Impacts

Thierry Roncalli*

*Amundi Asset Management[1]

*University of Paris-Saclay

November 2024

[1]The opinions expressed in this presentation are those of the authors and are not meant to represent the opinions or official positions of Amundi Asset Management.

Agenda

Greenhouse effect

Figure 1: A glass house

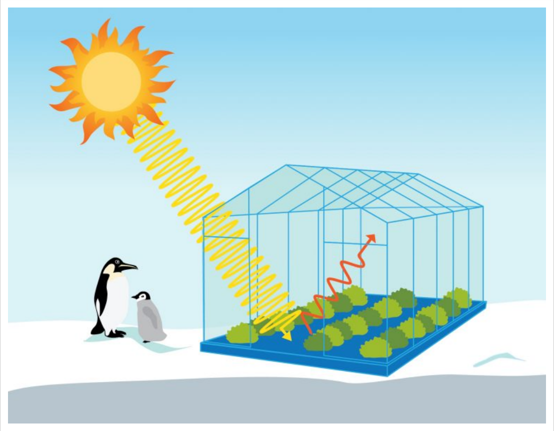

Greenhouse effect

The founding text of the greenhouse effect is a French scientific publication written by Joseph Fourier in 1824: *Remarques générales sur les températures du globe terrestre et des espaces planétaires*[2]:

> *"The heat of the Earth's surface derives from three sources, which must first be distinguished:*
>
> 1. *The Earth is heated by the sun's rays, whose uneven distribution produces the diversity of climates.*
> 2. *The Earth's temperature depends on the common temperature of planetary spaces, as it is exposed to the irradiation of the innumerable stars that surround the solar system on all sides.*
> 3. *The earth has retained within its mass some of the primitive heat it contained when the planets were formed."*

[2] *General Remarks on Global and Planetary Temperatures.*

Greenhouse effect

- In 1859, **Tyndall showed that water vapor has a high heat absorption capacity**. He went on to show that carbon dioxide and other gases could also absorb and radiate heat. Tyndall is the first scientist to prove that greenhouse gases exist and are responsible for the greenhouse effect
- Three years earlier, in 1856 and 1857, the American scientist Eunice Newton Foote had published two research papers with experiments showing that **water vapor and carbon dioxide absorb heat from solar radiation**
- Svante Arrhenius was the first scientist to calculate the effect of a change in atmospheric CO_2 on ground temperature (1896) $\Rightarrow$ **climate sensitivity**

Greenhouse effect

Figure 2: Diagram showing how the greenhouse effect works

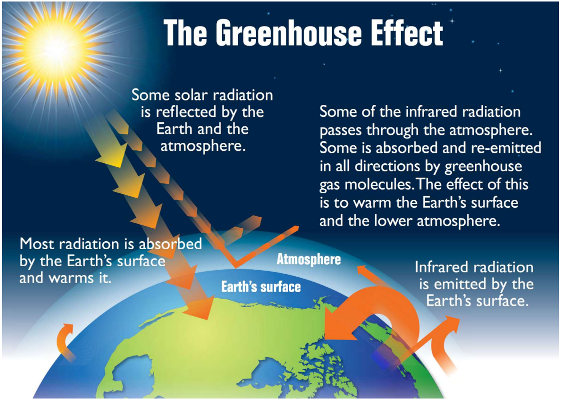

Source: US EPA (2012),
https://energyeducation.ca/encyclopedia/Greenhouse_effect.

Greenhouse effect

Figure 3: The pioneers of the greenhouse effect

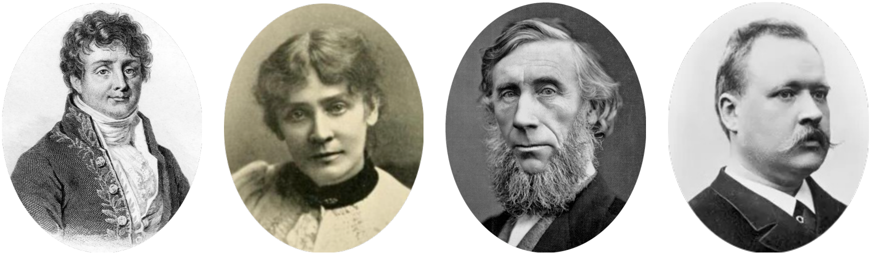

Joseph Fourier (1766–1830) | Eunice Newton Foote (1819–1888) | John Tyndall (1820–1893) | Svante Arrhenius (1859–1927)

Greenhouse effect

Table 1: List of greenhouse gases

Greenhouse gas	Formula	Kyoto Protocol
Water vapor	H_2O	
Carbon dioxide	CO_2	✓
Methane	CH_4	✓
Nitrous oxide	N_2O	✓
Ozone	O_3	
	Fluorinated or F-gases	
Sulfur hexafluoride	SF_6	✓
Nitrogen trifluoride	NF_3	✓
Chlorofluorocarbons	CFCs (CFC-11, CFC-12, etc.)	
Hydrofluorocarbons	HFCs (HFC-23, HFC-32, etc.)	✓
Hydrochlorofluorocarbons	HCFCs (HCFC-12, etc.)	
Perfluorocarbons	PFCs (CF_4, C_2F_6, etc.)	✓

Global warming

Callendar Effect

*"**By fuel combustion man has added about 150 000 million tons of carbon dioxide to the air during the past half century**. The author estimates from the best available data that approximately three quarters of this has remained in the atmosphere. The radiation absorption coefficients of carbon dioxide and water vapour are used to show the effect of carbon dioxide on sky radiation. From this the increase in mean temperature, due to the artificial production of carbon dioxide, is estimated to be at the rate of* $0.003°\mathrm{C}$ *per year at the present time. The temperature observations at zoo meteorological stations are used to show that world temperatures have actually increased at an average rate of* $0.005°\mathrm{C}$ *per year during the past half century." (Callendar, 1938, page 223).*

Collected papers on global warming by David Archer and Raymond Pierrehumbert

- 1824
  On the Temperatures of the Terrestrial Sphere and Interplanetary Space (Fourier)
- 1861
  On the Absorption and Radiation of Heat by Gases and Vapours, and on the Physical Connexion of Radiation, Absorption, and Conduction (Tyndall)
- 1896
  On the Influence of Carbonic Acid in the Air upon the Temperature of the Ground (Arrhenius)
- 1938
  The Artificial Production of Carbon Dioxide and its Influence on Temperature (Callendar)
- 1956
  The Influence of the 15μ Carbon-dioxide Band on the Atmospheric Infra-red Cooling Rate (Plass)
- 1957
  Carbon Dioxide Exchange Between Atmosphere and Ocean and the Question of an Increase of Atmospheric CO_2 during the Past Decades (Revelle and Suess)
- 1958
  Distribution of Matter in the Sea and Atmosphere: Changes in the Carbon Dioxide Content of the Atmosphere and Sea due to Fossil Fuel Combustion (Bolin and Eriksson)
- 1960
  The Concentration and Isotopic Abundances of Carbon Dioxide in the Atmosphere (Keeling)

Collected papers on global warming by David Archer and Raymond Pierrehumbert

- 1967
  Thermal Equilibrium of the Atmosphere with a Given Distribution of Relative Humidity (Manabe and Wetherald)
- 1969
  The Effect of Solar Radiation Variations on the Climate of the Earth (Budyko)
  A Global Climatic Model Based on the Energy Balance of the Earth-Atmosphere System (Sellers)
- 1970
  Is Carbon Dioxide from Fossil Fuel Changing Man's Environment? (Keeling)
- 1972
  Man-Made Carbon Dioxide and the Greenhouse Effect (Sawyer)
- 1975
  The Effects of Doubling the CO_2 Concentration on the Climate of a General Circulation Model (Manabe and Wetherald)
- 1977
  Changes of Land Biota and Their Importance for the Carbon Cycle (Bolin)
  Neutralization of Fossil Fuel CO_2 by Marine Calcium Carbonate (Broecker and Takahashi)
- 1979
  Carbon Dioxide and Climate: A Scientific Assessment (Charney, Arakawa, Baker *et al.*)
- 1984
  Climate Sensitivity: Analysis of Feedback Mechanisms (Hansen, Lacis, Rind *et al.*)

Global warming

Figure 4: Keeling curve: monthly mean CO_2 concentration in Mauna Loa

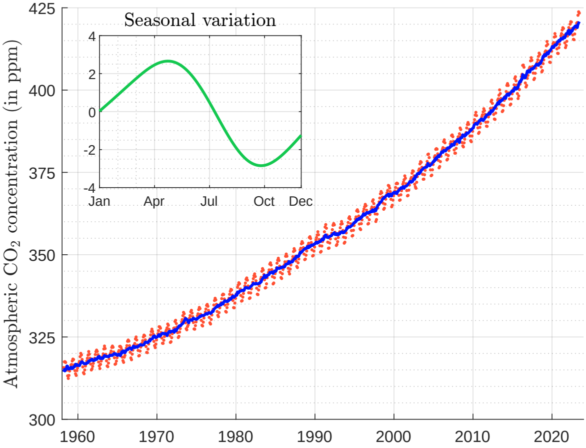

Source: Keeling *et al.* (2001) and `https://scrippsco2.ucsd.edu`.

Global warming

Charney Report (1979)

On July 23-27, 1979, Jule Charney formed a study group to "*assess the scientific basis for projection of possible future climatic changes resulting from man-made releases of carbon dioxide into the atmosphere*". The study group had 13 members, including eminent scientists Akio Arakawa, Bert Bolin, Henry Stommel, etc. The report examined the results of five global climate models that simulate the climatic response to an increase in atmospheric CO2: three by Manabe and his colleagues at NOAA's Geophysical Fluid Dynamics Laboratory and two by James Hansen and his colleagues at NASA's Goddart Institute for Space Studies. The report estimated a climate sensitivity of $3^\circ\mathrm{C}$, with an error of $\pm 1.5^\circ\mathrm{C}$.

Global warming

Figure 5: The fathers of the concept of global warming

Guy Stewart Callendar
(1898–1964)

Roger Revelle
(1909–1991)

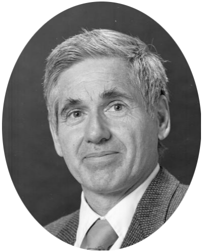

Charles David Keeling
(1928–2005)

Wallace Broecker
(1931–2019)

Global warming

Testimony of James Hansen to the US Senate (1988)

"Mr. Chairman and committee members, thank you for the opportunity to present the results of my research on the greenhouse effect which has been carried out with my colleagues at the NASA Goddard Institute for Space Studies. I would like to draw three main conclusions. Number one, the earth is warmer in 1988 than at any time in the history of instrumental measurements. Number two, the global warming is now large enough that we can ascribe with a high degree of confidence a cause and effect relationship to the greenhouse effect. And number three, our computer climate simulations indicate that the greenhouse effect is already large enough to begin to affect the probability of extreme events such as summer heat waves."

Global warming

In 1988, the United Nations Environment Programme (UNEP) and the World Meteorological Organization (WMO) established the **Intergovernmental Panel on Climate Change (IPCC)** to provide policy makers with regular scientific assessments of climate change, its impacts and potential future risks, and to recommend options for adaptation and mitigation

Definition

- The **Anthropocene** is a proposed geological epoch that dates from the beginning of significant human impacts on Earth's geology and ecosystems, including but not limited to human-induced climate change
- The term Anthropocene was popularized by Paul Crutzen[3] and Eugene Stoermer[4] in 2000 (Crutzen and Stoermer, 2000)

---

[3]Paul Crutzen (1933-2021) was awarded the 1995 Nobel Prize in Chemistry for his work in atmospheric chemistry, and in particular for his efforts to study the formation and decomposition of atmospheric ozone.

[4]Eugene Stoermer (1934-2012) was a professor of biology who specialized in the study of freshwater species and diatoms.

Definition

Figure 6: Geologic time scale

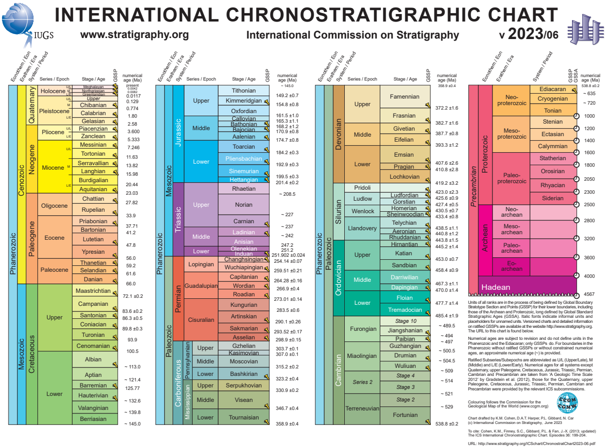

Source: International Commission on Stratigraphy (2023),

Geological history of the climate

Table 2: Units of time

Symbol	Definition	(in year)	Symbol	Name
Kyr/kyr	Thousand/Kilo years	10^3	ka	Kiloannus
Myr/myr	Mega/Million years	10^6	Ma	Megaannus
Gyr/byr	Giga/Billion years	10^9	Ga	Gigaannus

Geological history of the climate

- To estimate temperatures during the Precambrian, scientists use indirect methods, including geochemical proxies (chemical properties of rocks and minerals), paleontological studies (type and distribution of fossils and sedimentary rocks), and general circulation models.
- One of the most common methods is the clumped isotope thermometer
- The ratio of the two carbon isotopes $^{12}\mathrm{C}$ and $^{13}\mathrm{C}$ is:

$$\delta^{13}\mathrm{C} = 1000 \times \left(\left. \frac{^{13}\mathrm{C}}{^{12}\mathrm{C}}_{\text{sample}} \right/ \frac{^{13}\mathrm{C}}{^{12}\mathrm{C}}_{\text{standard}} - 1 \right)$$

  The unit of $\delta^{13}\mathrm{C}$ is parts per thousand
- Faint young Sun paradox
- Snowball Earth hypothesis

Geological history of the climate

Figure 7: Carbon isotopic evolution of marine carbonate

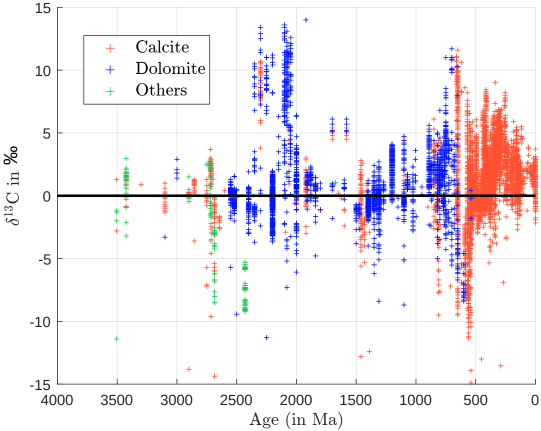

Source: Shields and Veizer (2002, Figure 2, page 5) & `https://earthref.org/ERDA/48`.

Geological history of the climate

Figure 8: Neoproterozoic carbon isotope data compilation

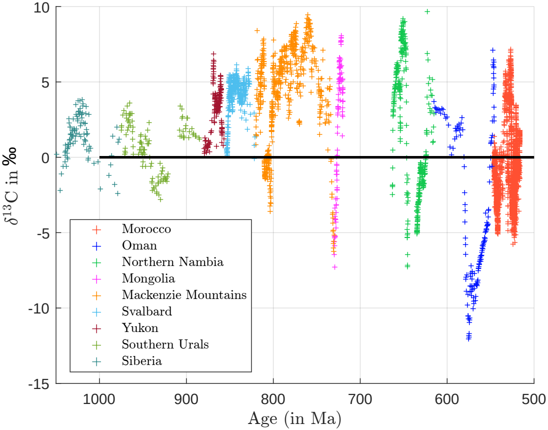

Source: Cox *et al.* (2016, Figure 2, page 90).

Geological history of the climate

Figure 9: Cosmic calendar

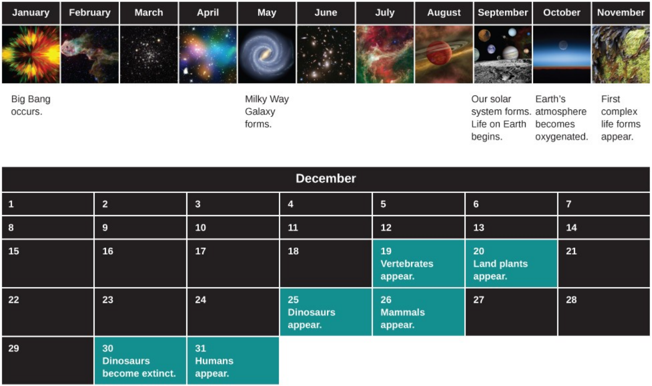

Source: `https://courses.lumenlearning.com/suny-astronomy/chapter/a-conclusion-and-a-beginning`.

Geological history of the climate

Temperature scales

- Three different scales are commonly used to measure temperature: Celsius, Kelvin, and Fahrenheit
- Their symbols are $^{\circ}\mathrm{C}$, K, and $^{\circ}\mathrm{F}$
- The relationships between the Celsius and Kelvin scales are $\mathcal{T}_{^{\circ}\mathrm{C}} = \mathcal{T}_{\mathrm{K}} - 273.15$ and $\mathcal{T}_{\mathrm{K}} = \mathcal{T}_{^{\circ}\mathrm{C}} + 273.15$.
- For Celsius and Fahrenheit, we have $\mathcal{T}_{^{\circ}\mathrm{C}} = \frac{5}{9}\left(\mathcal{T}_{^{\circ}\mathrm{F}} - 32\right)$ and $\mathcal{T}_{^{\circ}\mathrm{F}} = \frac{9}{5}\mathcal{T}_{^{\circ}\mathrm{F}} + 32$
- Absolute zero is $-273.15^{\circ}\mathrm{C}$, $0\,\mathrm{K}$ and $-459.67^{\circ}\mathrm{F}$, implying that $\mathcal{T} \geq -273.15^{\circ}\mathrm{C}$, $\mathcal{T} \geq 0\,\mathrm{K}$, and $\mathcal{T} \geq -459.67^{\circ}\mathrm{F}$
- The melting point (at standard pressure) is obtained at temperatures of $0^{\circ}\mathrm{C}$, $273.15\,\mathrm{K}$ and $32^{\circ}\mathrm{F}$
- The boiling point of water corresponds to temperatures of $100^{\circ}\mathrm{C}$, $373.15\,\mathrm{K}$ and $212^{\circ}\mathrm{F}$

Palaeoclimate during the Phanerozoic

Figure 10: Earth temperature since 500 Myr BP (°C vs. 1960-1990 average)

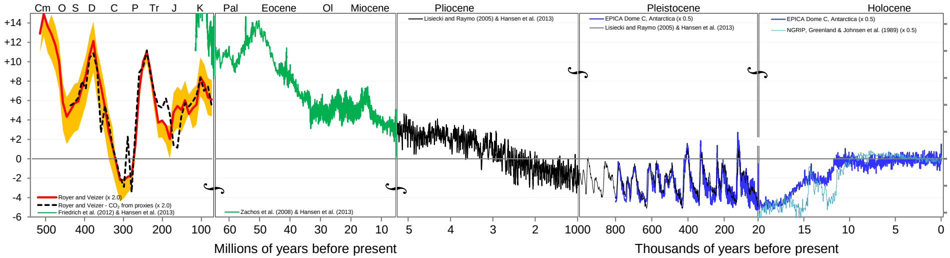

Palaeoclimate during the Phanerozoic

Table 3: Recovered deep and very deep ice cores

Greenland			Antarctica		
Site 2	1956	305 m	Byrd Station	1957-1958	307 m
Site 2	1957	411 m	Little America	1958-1959	264 m
Camp Century	1961-1966	1387 m	Byrd Station	1966-1968	2164 m
Dye 3	1971	372 m	Vostock	1990-1998	3623 m
Milcent	1973	398 m	Dome Fuji	1994-1997	2503 m
Crete	1974	405 m	Vostock	2005-2007	**3658 m**
Dye 3	1979-1981	2037 m	Dome Fuji	2003-2007	3035 m
GRIP	1989-1992	3029 m	Dome C	1999-2005	3270 m
GISP 2	1989-1993	3057 m	Kohnen Station	2001-2006	2774 m
NGRIP	1996-2004	3090 m	WAIS	2006-2011	3405 m

Palaeoclimate during the Phanerozoic

Figure 11: Greenland deep drilling sites

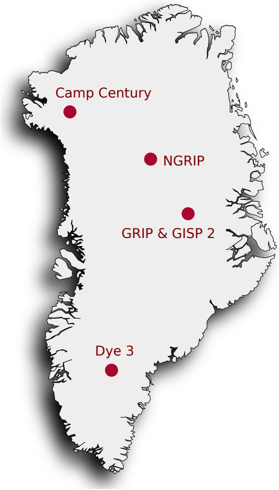

Palaeoclimate during the Phanerozoic

Figure 12: Antarctica deep drilling sites

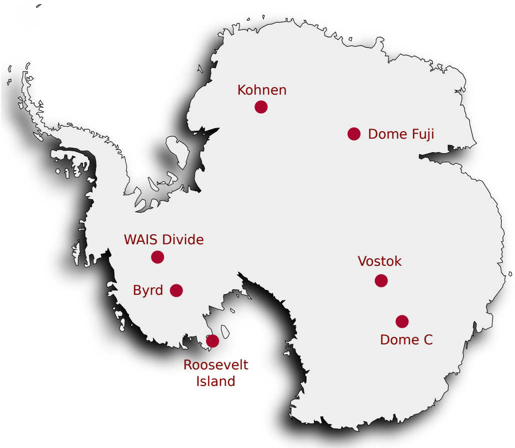

Palaeoclimate during the Phanerozoic

Table 4: Isotopes of chemical elements

Element	Stable isotopes	Unstable isotopes	Major isotope
Hydrogen	${}^{1}_{1}\mathrm{H}$ and ${}^{2}_{1}\mathrm{H}$	${}^{3}_{1}\mathrm{H}$ – ${}^{7}_{1}\mathrm{H}$	Protium (99.98%)
Carbon	${}^{12}_{6}\mathrm{C}$ and ${}^{13}_{6}\mathrm{C}$	${}^{8}_{6}\mathrm{C}$ – ${}^{11}_{6}\mathrm{C}$ and ${}^{14}_{6}\mathrm{C}$ – ${}^{22}_{6}\mathrm{C}$	Carbon-12 (98.90%)
Oxygen	${}^{16}_{8}\mathrm{O}$ and ${}^{18}_{8}\mathrm{O}$	${}^{17}_{8}\mathrm{O}$ and ${}^{19}_{8}\mathrm{O}$ – ${}^{27}_{8}\mathrm{O}$	Oxygen-16 (99.76%)
Uranium		${}^{232}_{92}\mathrm{U}$ – ${}^{242}_{92}\mathrm{U}$	Uranium-238 (99.27%)

Palaeoclimate during the Phanerozoic

- Analysis of trapped air bubbles in ice cores provides a direct record of the composition of the atmosphere at the time the ice formed
- Dansgaard (1964) defined the relative deviation δ of the heavy isotope content as follows:

$$\delta = 1000 \times \left(\frac{R_{\mathrm{sample}} - R_{\mathrm{standard}}}{R_{\mathrm{standard}}} \right)$$

  where R is the absolute content
- δ is measured in ‰
- As the chemical formula of water is H_2O, climate reconstruction from ice cores is based on the analysis of hydrogen and oxygen
  - In the case of hydrogen, the common isotope is $^{1}\mathrm{H}$, while the heavy isotope is $^{2}\mathrm{H}$ (also called the deuterium or D)
  - The ratio R is then $\dfrac{^{2}\mathrm{H}}{^{1}\mathrm{H}}$ and the relative variation is written as $\delta\mathrm{D}$
  - In the case of oxygen, the common isotope is $^{16}\mathrm{O}$, while the heavy isotope is $^{18}\mathrm{O}$
  - The ratio R is then $\dfrac{^{18}\mathrm{O}}{^{16}\mathrm{O}}$ and the relative variation is written as $\delta^{18}\mathrm{O}$

Palaeoclimate during the Phanerozoic

Figure 13: Part of an ice core at WAIS Divide Field Camp

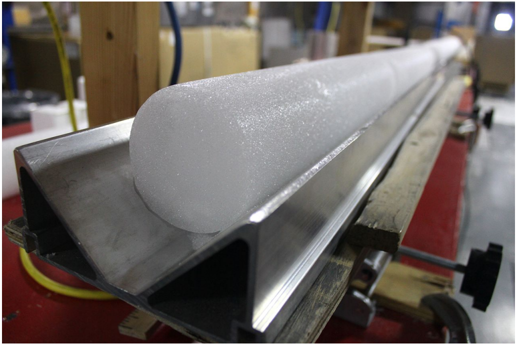

Source: Eli Duke, Antarctica: WAIS Divide Field Camp (Flickr), www.flickr.com/photos/80547277@N00/9518403333.

Palaeoclimate during the Phanerozoic

- The aim of ice core analysis is to estimate the temperature function $t \longmapsto \mathcal{T}(t)$ with respect to the time age t
- The raw analysis provides two measurements: the depth d of the ice core drilling and the isotope ratio measure δ
- We therefore observe the isotope function $d \longmapsto \delta(d)$
- To obtain the temperature function, we proceed in two steps:
  1. First, we transform the depth d of the ice core drilling into the time age t:
  $$t = \varphi_t(d)$$
  2. We then estimate the temperature $\mathcal{T}$ associated with the isotope ratio $\delta(d)$:
  $$\mathcal{T} = \varphi_{\mathcal{T}}(\delta(d))$$
- Combining the two previous equations gives the desired parametric function $t \longmapsto \mathcal{T}(t)$

Palaeoclimate during the Phanerozoic

Figure 14: Isotopic reconstruction of Vostok ice cores

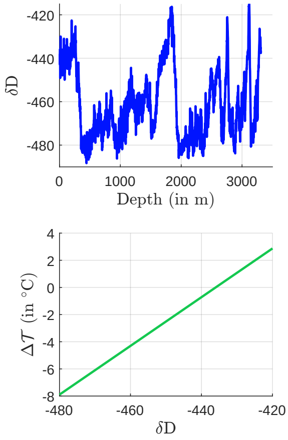

Source: Petit *et al.* (1999) & Author's calculations.

Palaeoclimate during the Phanerozoic

Figure 15: Temperature reconstruction of Vostok ice cores

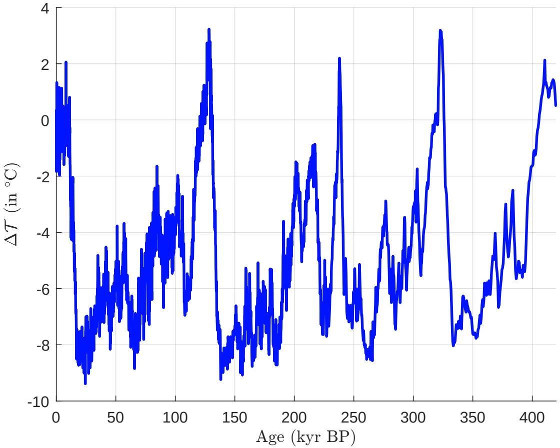

Source: Petit *et al.* (1999).

Palaeoclimate during the Phanerozoic

Figure 16: Gas concentration of Vostok ice cores

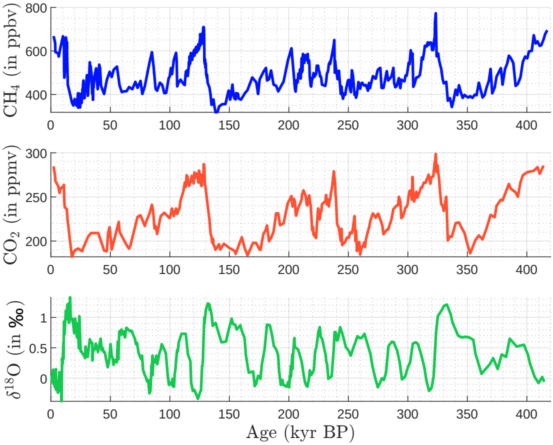

Source: Petit *et al.* (1999).

Palaeoclimate during the Phanerozoic

Figure 17: Evolution of the atmospheric CO_2 during the last 420 million years

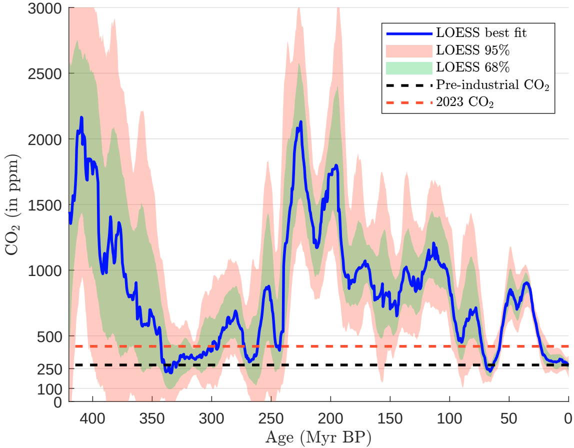

Source: Foster *et al.* (2017, Figure 1, page 3).

Anthropogenic factors of climate change

Temperature anomaly

We define the temperature anomaly at time t as the difference between the temperature at time t and the temperature for a reference period:

$$\Delta\mathcal{T}(t) = \mathcal{T}(t) - \mathcal{T}_{\mathfrak{B}ase}$$

where $\mathcal{T}_{\mathfrak{B}ase}$ is the reference temperature. It is generally the average of the temperature of the reference period:

$$\mathcal{T}_{\mathfrak{B}ase} = \frac{\sum_{j \in \mathfrak{B}ase} \mathcal{T}(j)}{n_{\mathfrak{B}ase}}$$

For example, the reference temperature can be the average temperature of the 20th century (from 1901 to 2000) or the pre-industrial period

Temperature anomaly

Figure 18: Global average land-ocean temperature anomaly relative to 1961-1990 average

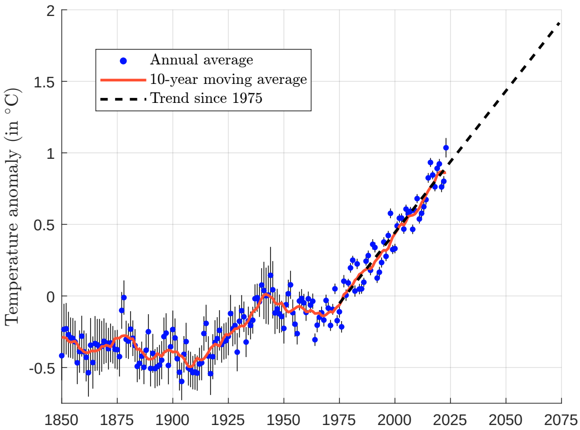

Source: Morice *et al.* (2021).

Temperature anomaly

Figure 19: Average land-ocean temperature anomaly in the northern and southern hemispheres relative to the 1961-1990 average

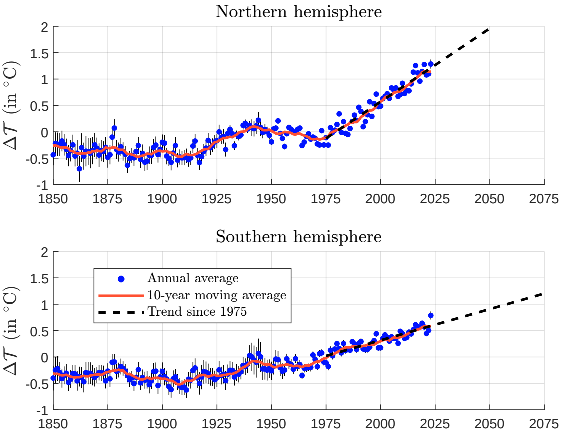

Source: Morice *et al.* (2021).

Temperature anomaly

Table 5: Linear projection of land-ocean temperature anomaly (in $^\circ\mathrm{C}$)

Year	HadCRUT5			NOAAGlobalTemp v5.1		
	Global	Northern	Southern	Global	Northern	Southern
2050	1.4336	1.9595	0.9078	1.4576	1.9894	0.9247
2075	1.9288	2.6540	1.2035	1.9185	2.6715	1.1642
2100	2.4239	3.3486	1.4992	2.3795	3.3536	1.4038
Slope	0.0198	0.0278	0.0118	0.0184	0.0273	0.0096

Source: NOAAGlobalTemp v5.1 & Author's calculations.

Table 6: Linear projection of land and ocean temperature anomalies (in $^\circ\mathrm{C}$)

Year	Global		Northern		Southern	
	Land	Ocean	Land	Ocean	Land	Ocean
2050	2.4212	1.0238	2.8388	1.3482	1.4719	0.7972
2075	3.2386	1.3243	3.8176	1.8061	1.9222	0.9875
2100	4.0560	1.6247	4.7964	2.2641	2.3725	1.1779
Slope	0.0327	0.0120	0.0392	0.0183	0.0180	0.0076

Source: NOAAGlobalTemp v5.1 & Author's calculations.

Temperature anomaly

Figure 20: Average temperature anomaly (land-ocean, land and ocean)

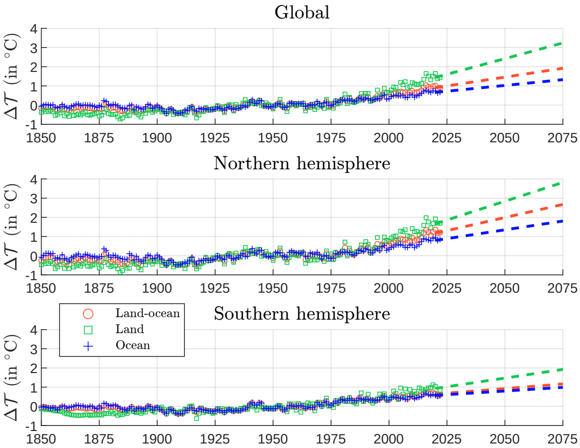

Source: Vose *et al.* (2021).

Temperature anomaly

Figure 21: Projection of temperature anomaly by 2100 (in $^\circ\mathrm{C}$)

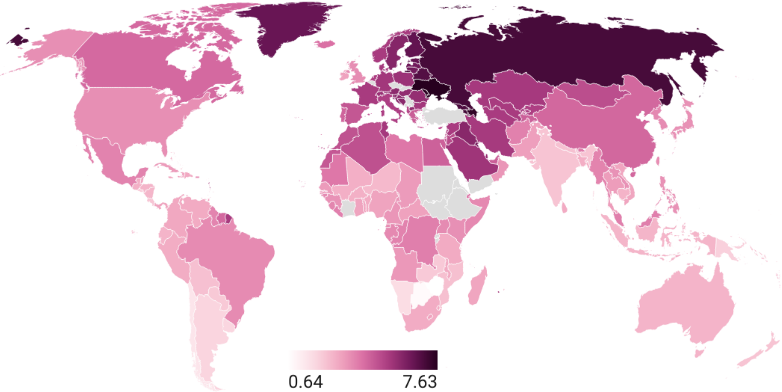

Source: `https://www.fao.org/faostat/en/#data/ET` & Author's calculations.

Anthropogenic GHG emissions

Carbon budget

- According to Friedlingstein *et al.* (2022), the global carbon budget has five main components:
  1. Fossil fuel combustion and oxidation from all energy and industrial processes, including cement production and carbonation ($\mathcal{CE}_{\mathrm{Industry}}$)
  2. Emissions from land-use change ($\mathcal{CE}_{\mathrm{Land}}$)
  3. The growth rate of atmospheric CO_2 concentration ($\mathcal{CE}_{\mathrm{AT}}$)
  4. The uptake of CO_2 by the oceans (ocean sink) ($\mathcal{CS}_{\mathrm{Ocean}}$)
  5. The uptake of CO_2 by the land (land sink) ($\mathcal{CS}_{\mathrm{Land}}$)
- From a theoretical point of view, we have the following identity:

$$\mathcal{CE}_{\mathrm{AT}} = \underbrace{\left(\mathcal{CE}_{\mathrm{Industry}} + \mathcal{CE}_{\mathrm{Land}}\right)}_{\text{Positive emissions}} - \underbrace{\left(\mathcal{CS}_{\mathrm{Ocean}} + \mathcal{CS}_{\mathrm{Land}}\right)}_{\text{Negative emissions}}$$

- The estimated budget imbalance is equal to:

$$\mathcal{CB}_{\mathrm{Imbalance}} = \mathcal{CE}_{\mathrm{Industry}} + \mathcal{CE}_{\mathrm{Land}} - \left(\mathcal{CE}_{\mathrm{AT}} + \mathcal{CS}_{\mathrm{Ocean}} + \mathcal{CS}_{\mathrm{Land}}\right)$$

Anthropogenic GHG emissions

- In 2021, the authors estimate the following figures expressed in gigatonnes of carbon: $\mathcal{CE}^{\star}_{\mathrm{Industry}} = 10.13$, $\mathcal{CE}_{\mathrm{Land}} = 1.08$, $\mathcal{CE}_{\mathrm{AT}} = 5.23$, $\mathcal{CS}_{\mathrm{Ocean}} = 2.88$, $\mathcal{CS}_{\mathrm{Land}} = 3.45$, $\mathcal{CS}_{\mathrm{Cement}} = 0.23$, and $\mathcal{CB}_{\mathrm{Imbalance}} = -0.58$
- Expressed in gigatonnes of CO_2 we obtain: $\mathcal{CE}^{\star}_{\mathrm{Industry}} = 37.12$, $\mathcal{CE}_{\mathrm{Land}} = 3.94$, $\mathcal{CE}_{\mathrm{AT}} = 19.14$, $\mathcal{CS}_{\mathrm{Ocean}} = 10.55$, $\mathcal{CS}_{\mathrm{Land}} = 12.64$, $\mathcal{CS}_{\mathrm{Cement}} = 0.84$, and $\mathcal{CB}_{\mathrm{Imbalance}} = -2.12$
- Anthropogenic CO_2 emissions are therefore **36.28** $\mathrm{GtCO_2}$ for industrial processes ($\mathcal{CE}_{\mathrm{Industry}}$) and **3.94** $\mathrm{GtCO_2}$ for land-use change
- Since the total is **40.22** $\mathrm{GtCO_2}$, 26.23% and 31.43% of the total anthropogenic CO_2 emissions have been absorbed by oceans and land, respectively, while **47.60% remain in the atmosphere**

Anthropogenic GHG emissions

Figure 22: Annual CO_2 emissions (in $\mathrm{GtCO_2}$)

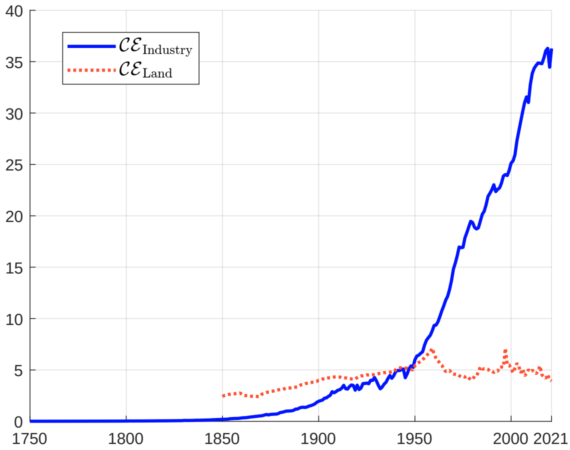

Source: Friedlingstein *et al.* (2022) & Author's calculations.

Anthropogenic GHG emissions

Figure 23: Cumulative CO_2 emissions and carbon sinks (in $\mathrm{GtCO_2}$)

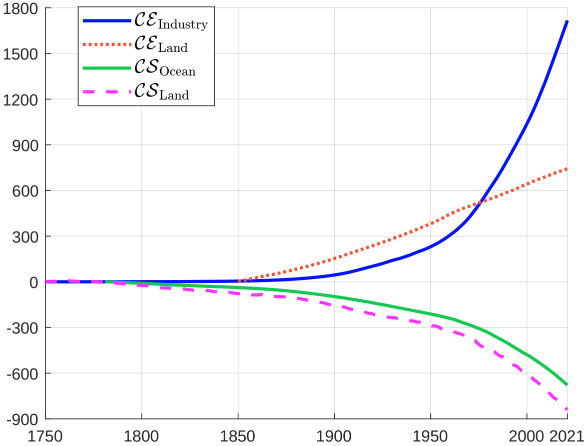

Source: Friedlingstein *et al.* (2022) & Author's calculations.

Anthropogenic GHG emissions

Figure 24: Cumulative CO_2 budget imbalance in atmosphere (in $\mathrm{GtCO_2}$)

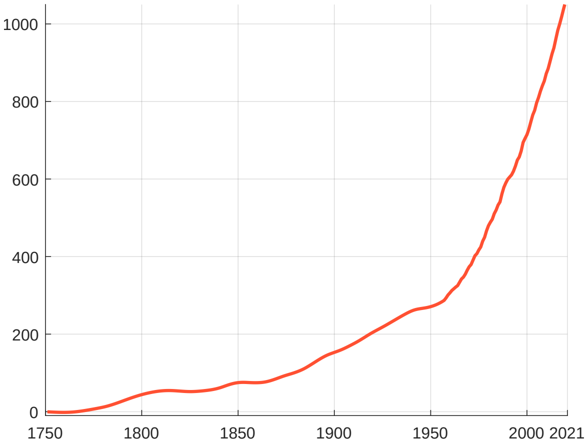

Source: Friedlingstein *et al.* (2022) & Author's calculations.

Anthropogenic GHG emissions

The **airbone fraction** is the ratio of the atmospheric CO_2 growth rate to total anthropogenic emissions. For the period 1750–2021, this ratio is equal to:

$$\mathrm{AF} = \frac{\mathcal{CE}_{\mathrm{AT}}}{\mathcal{CE}_{\mathrm{Industry}} + \mathcal{CE}_{\mathrm{Land}}} = \frac{1\,076}{1\,717 + 742} = 43.8\%$$

This means that 43.8% of anthropogenic emissions have not been absorbed by natural carbon sinks

> *"The observed stability of the airborne fraction over the 1960–2020 period indicates that the ocean and land CO_2 sinks have on average been removing about 55% of the anthropogenic emissions." (Friedlingstein et al., 2022, page 4834).*

Anthropogenic GHG emissions

Table 7: Breakdown of anthropogenic CO_2 emission by energy source (in %)

	Energy	1850	1900	1950	1975	2000	2020
Annual CO_2 emissions	Coal	100.00	95.85	65.10	34.74	36.18	40.11
	Oil	0.00	3.55	26.79	47.64	40.42	33.23
	Gas	0.00	0.60	6.09	13.17	18.61	20.38
	Cement	0.00	0.00	1.13	1.99	2.87	4.33
	Flaring	0.00	0.00	0.81	2.18	1.05	1.12
	Other	0.00	0.00	0.08	0.29	0.86	0.83
Cumulative CO_2 emissions	Coal	100.00	97.58	85.24	63.49	50.00	46.29
	Oil	0.00	2.05	12.13	27.43	35.10	35.02
	Gas	0.00	0.37	2.15	6.88	11.72	14.52
	Cement	0.00	0.00	0.40	1.17	1.77	2.56
	Flaring	0.00	0.00	0.03	0.87	1.03	1.06
	Other	0.00	0.00	0.06	0.16	0.39	0.55

Source: Friedlingstein *et al.* (2022) & Author's calculations.

Anthropogenic GHG emissions

Figure 25: Energy source breakdown of anthropogenic cumulative CO_2 (in %)

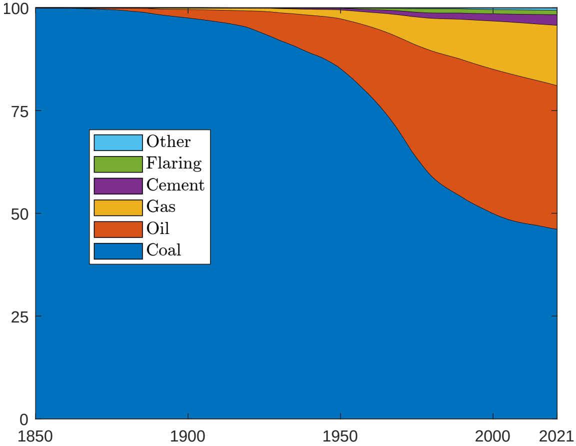

Source: Friedlingstein *et al.* (2022) & Author's calculations.

Anthropogenic GHG emissions

Figure 26: Share of CO_2 emissions by region (in % of total)

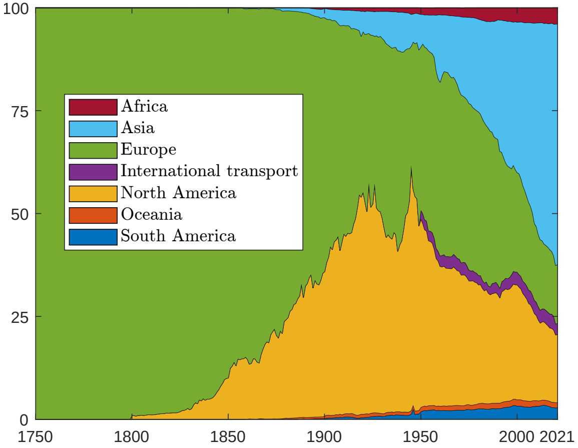

Source: Friedlingstein *et al.* (2022).

Anthropogenic GHG emissions

Figure 27: Share of cumulative CO_2 emissions by region (in % of total)

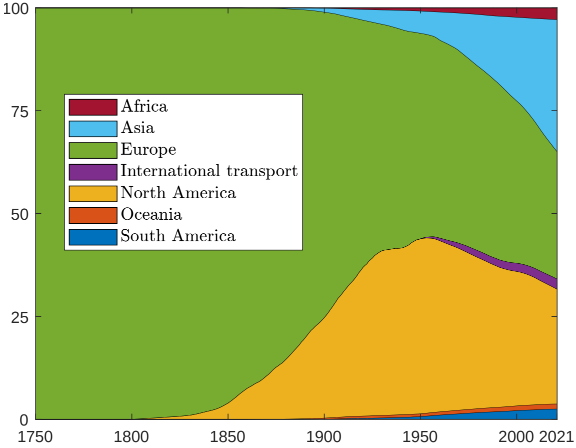

Source: Friedlingstein *et al.* (2022).

Anthropogenic GHG emissions

Figure 28: Share of CO_2 emissions by country (in % of total)

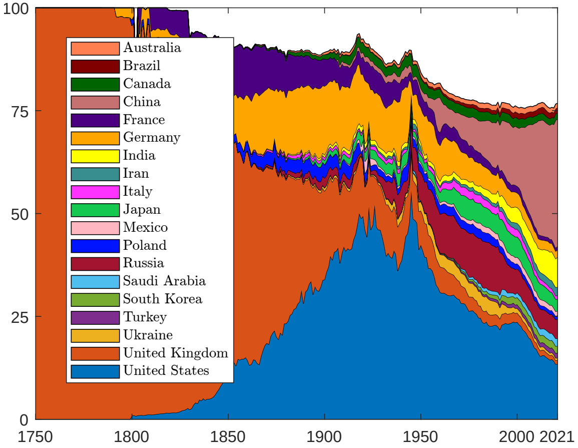

Source: Friedlingstein *et al.* (2022).

Anthropogenic GHG emissions

Figure 29: Share of cumulative CO_2 emissions by country (in % of total)

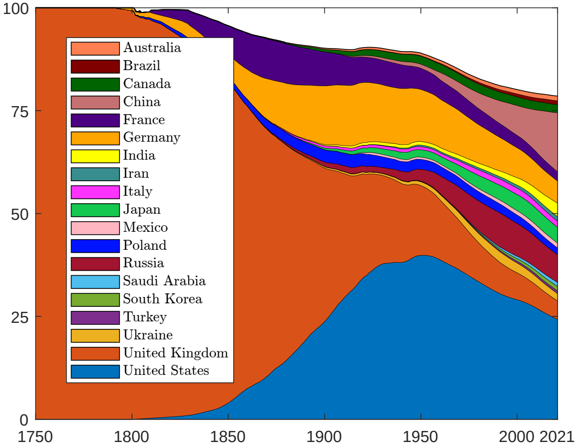

Source: Friedlingstein *et al.* (2022).

Anthropogenic GHG emissions

Kaya identity

The Kaya identity is defined as:

$$\text{Anthropogenic } CO_2 \text{ emissions} = \text{Population} \times \frac{\text{GDP}}{\text{Population}} \times \frac{\text{Energy}}{\text{GDP}} \times \frac{CO_2 \text{ emissions}}{\text{Energy}}$$

Using the notations of Kaya and Yokobori (1997), this identity is generally expressed as:

$$F = P \times \frac{G}{P} \times \frac{E}{G} \times \frac{F}{E}$$

Therefore, the key drivers of anthropogenic CO_2 emissions include four main factors:

1. the population (demographics)
2. the GDP per capita (economics)
3. the energy intensity of the GDP (engineering)
4. the carbon intensity (physics)

Anthropogenic GHG emissions

Figure 30: Key drivers of the Kaya identity

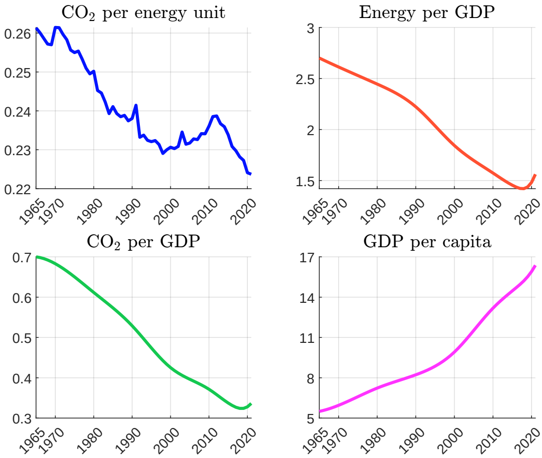

Source: Friedlingstein *et al.* (2022).

Anthropogenic GHG emissions

Figure 31: CO_2 emissions per capita (in $\mathrm{tCO_2}$ per person)

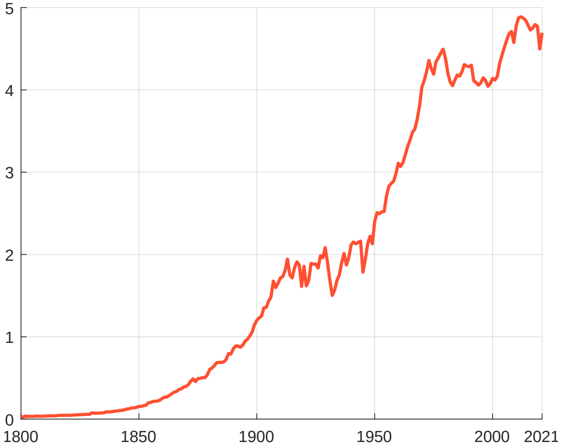

Source: Friedlingstein *et al.* (2022).

Anthropogenic GHG emissions

Figure 32: GHG emissions (in $GtCO_2e$)

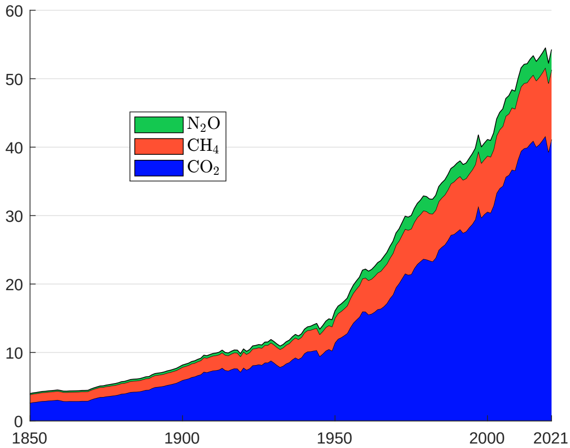

Source: Jones *et al.* (2023) & Author's calculations.

Anthropogenic GHG emissions

Table 8: 2021 greenhouse gas emissions (in $\mathrm{GtCO_2e}$)

CH_4			CO_2			N_2O		
$\mathcal{CE}_{\text{Industry}}$	$\mathcal{CE}_{\text{Land}}$	$\mathcal{CE}_{\text{Total}}$	$\mathcal{CE}_{\text{Industry}}$	$\mathcal{CE}_{\text{Land}}$	$\mathcal{CE}_{\text{Total}}$	$\mathcal{CE}_{\text{Industry}}$	$\mathcal{CE}_{\text{Land}}$	$\mathcal{CE}_{\text{Total}}$
6.23	3.95	**10.18**	37.11	4.00	**41.12**	0.79	2.18	**2.97**
(61.2%)	(38.8%)	(18.8%)	(90.3%)	(9.7%)	(75.8%)	(26.7%)	(73.3%)	(5.5%)

Source: Jones *et al.* (2023) & Author's calculations.

The Methane factor!

Planetary boundaries

Figure 33: Planetary boundaries

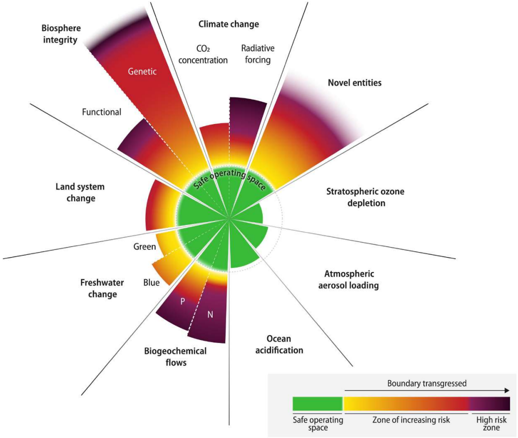

Source: Richardson *et al.* (2023, Figure 1, page 4).

Planetary boundaries

Table 9: Current status of planetary boundaries

No	Earth process system	Control variable	m_{1750}	m_{Boundary}	m_{upper}	m_{2023}	Crossed
1	Climate change	Atmospheric CO_2 concentration (ppm)	280	350	450	417	✓
		Atmospheric radiative forcing $(\mathrm{W/m^2})$	0	1.0	1.5	2.91	✓
2	Biodiversity loss	Genetic diversity (E/MSY)	1	10	100	> 100	✓
		Functional integrity (% HANPP)	1.9	10	20	30	✓
3	Stratospheric ozone depletion	Stratospheric O_3 concentration (DU)	290	276	261	284.6	
4	Ocean acidification	Carbonate ion concentration (Ω_{arg})	3.44	2.752	2.75	2.8	
5	Biogeochemical flows	Phosphate flow (TgP/yr) – global	0	11	100	22.6	✓
		Phosphate flow (TgP/yr) – regional	0	6.2	11.2	17.5	✓
		Nitrogen flow (TgN/yr)	0	62	82	190	✓
6	Land-use change	Area of forested land (%) – global	100	75	54	60	✓
		% area remaining – tropical	100	85	60	58.6	✓
		% area remaining – temperate	100	50	30	41.1	✓
		% area remaining – boreal	100	85	60	63.5	✓
7	Freshwater change	Blue water (%)	9.4	10.2	50	18.2	✓
		Green water (%)	9.8	11.1	50	15.8	✓
8	Atmospheric aerosol loading	Inter-hemispheric difference (AOD)	0.03	0.10	0.25	0.076	
9	Novel entities	Synthetic chemicals (%)	0	0	NA	> 0	✓

Source: Richardson *et al.* (2023, Table 1, pages 4-5).

First law of thermodynamics

"Temperature [...] is a measure of the energy contained in the movement of molecules. Therefore, to understand how the temperature is maintained, one must consider the energy balance that is formally stated in the first law of thermodynamics. The basic global energy balance of Earth is between energy coming from the Sun and energy returned to space by Earth's radiative emission. The generation of energy in the interior of Earth has a negligible influence on its energy budget." (Hartmann, 2016, page 25).

- **Energy cannot be created or destroyed** (law of conservation of energy)
- The total amount of energy in a closed system is conserved
- Energy and forcing are two interchangeable terms, meaning that $F_{\text{solar}} := \mathcal{E}_{\text{solar}}$, $F_{\text{thermal}} := \mathcal{E}_{\text{infrared}}$, etc.

Total solar irradiance

- The total amount of electromagnetic energy emitted by the Sun, also called the solar luminosity is $L_\odot = 3.828 \times 10^{26}$ watts
- **Total solar irradiance** (TSI) is defined as:

$$S_d = \frac{L_\odot}{4\pi d^2}$$

  where d is the distance of the sphere from the Sun in meters
- For the Earth, the distance is between 147.1 and 152.1 million kilometers
- Using a mean value of 149.6 million kilometers, we get:

$$S_0 = \frac{3.828 \times 10^{26}}{4\pi \left(149.6 \times 10^9\right)^2} = 1372.11 \ \mathrm{W/m}^2$$

- A direct measurement by astrophysicists gives 1368 $\mathrm{W/m}^2$

Planck law

Planck radiation law and spectral density of electromagnetic radiation

In physics, Planck's law describes the spectral distribution of electromagnetic radiation emitted by a black body in thermal equilibrium at a given temperature. The expression for the spectral density function is:

$$B_{\nu}\left(\nu, \mathcal{T}\right) = \frac{2h\nu^{3}}{c^{2}} \frac{1}{\exp\left(\dfrac{h\nu}{k\mathcal{T}}\right) - 1}$$

where $h = 6.62607015 \times 10^{-34}\,\mathrm{J\,Hz}^{-1}$ is Planck's constant, $c = 299\,792\,458\,\mathrm{m\,s}^{-1}$ is the speed of light in a vacuum, $k = 1.380649 \times 10^{-23}\,\mathrm{J\,K}^{-1}$ is Boltzmann's constant, $\mathcal{T}$ is the temperature measured in Kelvin, and ν is the frequency in hertz

Planck law

Planck law can be written in terms of the wavelength λ:

$$\lambda = \frac{c}{\nu} \qquad \left(\sim \frac{\mathrm{m\,s^{-1}}}{\mathrm{Hz}} = \mathrm{m} \right)$$

and we have:

- **Ultraviolet** wavelength: less than 380 nm
- Visible wavelength: 380 nm to 780 nm
- **Infrared** wavelength: greater than 780 nm

Planck law

Figure 34: Spectral density function $B_\lambda(\lambda, \mathcal{T})$ (in $10^{12}\ \mathrm{W/m^2\,m^{-1}}$)

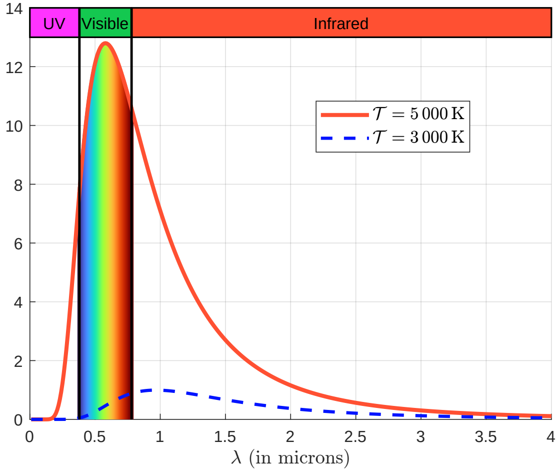

Planck law

Figure 35: Comparison of the radiation spectra of sunlight and the Earth's surface (in $10^{12}\ \mathrm{W/m^2\,m^{-1}}$)

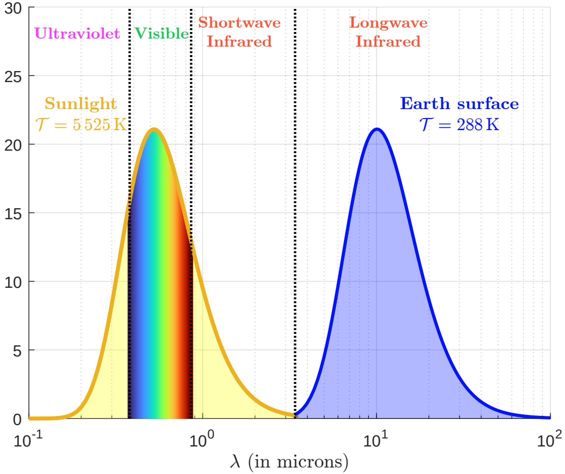

Stefan-Boltzmann law

Stefan-Boltzmann law

The Stefan-Boltzmann law describes the relationship between the total amount of radiation $\boldsymbol{\mathcal{E}}$ emitted by a body and its temperature $\mathcal{T}$:

$$\boldsymbol{\mathcal{E}} = \varepsilon \sigma \mathcal{T}^4$$

where:

- $\varepsilon \in [0, 1]$ is the emissivity of the body
- $\sigma = 5.67 \times 10^{-8}\ \mathrm{W/m^2\,K^{-4}}$ is the Stefan-Boltzmann constant
- For an ideal black body, we have $\varepsilon = 1$

Effective temperature of stars

- The radius of the Sun $R_\odot$ is about 696 342 kilometers
- The solar irradiance at the photosphere is equal to:

$$S_\odot = \frac{L_\odot}{4\pi R_\odot^2} = \frac{3.828 \times 10^{26}}{4\pi \left(696\,342 \times 10^3\right)^2} = 62\,822\,741 \ \mathrm{W/m^2}$$

- If we assume that the sun is a perfect black body ($\varepsilon \approx 0.96$), we have:

$$\sigma \mathcal{T}_\odot^4 = S_\odot \Leftrightarrow \mathcal{T}_\odot = \sqrt[4]{\frac{S_\odot}{\sigma}}$$

- We have:

$$\mathcal{T}_\odot = \sqrt[4]{\frac{62\,822\,741}{5.67 \times 10^{-8}}} = 5\,769\,\mathrm{K}$$

Effective temperature of stars

Remark

The previous analysis can be extended to other stars. Let R_{star} be the stellar radius of the star. Since we have $L_{\mathrm{star}} = 4\pi R_{\mathrm{star}}^2 S_{\mathrm{star}}$ and $S_{\mathrm{star}} = \mathcal{E} = \sigma \mathcal{T}^4$, we get:

$$\mathcal{T}_{\mathrm{star}} = \sqrt[4]{\frac{L_{\mathrm{star}}}{4\pi R_{\mathrm{star}}^2 \sigma}}$$

$\mathcal{T}_{\mathrm{star}}$ is defined as the temperature of a black body radiating the same amount of energy per unit area as the star. It may differ from the actual temperature of a star, which depends on its kinetic energy.

Incoming solar radiation

- The incoming solar radiation is equal to:

$$F_{\mathrm{solar}} = \frac{1}{4}\left(1 - \alpha_p\right) S_0$$

  where α_p is the planetary albedo, which measures the amount of reflected sunlight
- α_p is equal to zero for a perfect black body
- α_p one for a perfect white body

Remark

The ratio $\frac{1}{4}$ comes from the fact that no point on the planet receives the sun's energy continuously during a full day. On average, we can show that a point on the planet receives $\frac{1}{4}$ of the solar energy, which is the ratio of the projected area of the sphere ($\mathcal{A}rea = \pi r^2$) divided by the surface area of the sphere ($\mathcal{A}rea = 4\pi r^2$)

Incoming solar radiation

Figure 36: Incoming solar radiation

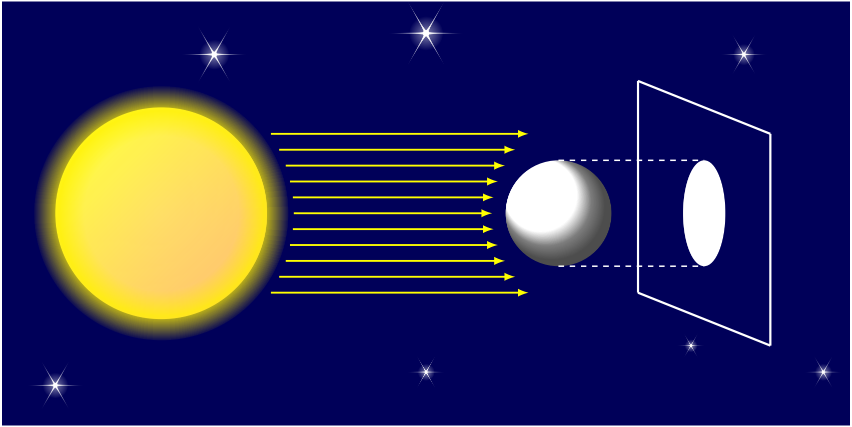

Incoming solar radiation

In the case of the Earth, we have $\alpha_p \approx 0.29$ and:

$$F_{\mathrm{solar}} = \frac{1}{4}(1 - 0.29) \times 1\,368 = 242.82 \mathrm{~W/m^2}$$

Incoming solar radiation

Interpretation

Consider a room with a surface area of x square meters and receiving an energy $\mathcal{E}$ expressed in watts. The radiation per square meter received by this room is equal to $\mathcal{E}/x$. If the room receives the same equivalent solar radiation F_{solar}, the energy must be equal to:

$$\mathcal{E} = x \cdot F_{\mathrm{solar}}$$

Using a standard 200 watt lamp, we can calculate the number of lamps required to achieve the same equivalent solar radiation. The results are shown below:

x (in m^2)	1	5	10	20	50	100
$\mathcal{E}$ (in watts)	242.8	1 214	2 428	4 856	12 141	24 282
# lights	1.2	9	12	24	61	121

For a room of 20 m^2, we need 24 lights.

Zero-order model of the atmosphere

Figure 37: Zero-order model

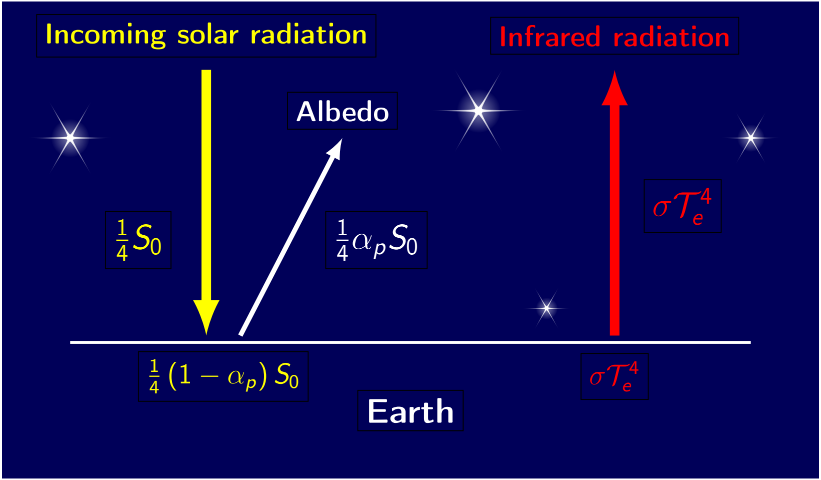

Effective temperature of the Earth

- The Earth receives the incoming solar radiation F_{solar}, while the black body radiation is given by the Stefan-Boltzmann law
- We deduce that:

$$\sigma \mathcal{T}_e^4 = \frac{1}{4} \left(1 - \alpha_p\right) S_0 \Leftrightarrow \mathcal{T}_e = \sqrt[4]{\frac{\left(1 - \alpha_p\right) S_0}{4\sigma}}$$

- The numerical calculation gives:

$$\begin{aligned} \mathcal{T}_e &= \sqrt[4]{\frac{(1 - 0.29) \times 1\,368}{4 \times 5.67 \times 10^{-8}}} \\ &= 255.81\,\mathrm{K} \\ &= 255.81^{\circ}\mathrm{C} - 273.15^{\circ}\mathrm{C} \\ &= -17.34^{\circ}\mathrm{C} \end{aligned}$$

- The effective temperature of the Earth is then close to $-17.34^{\circ}\mathrm{C}$

Effective temperature of the Earth

Without greenhouse gases, the surface temperature of the Earth should be equal to the effective temperature. However, we observe:

$$\mathcal{T}_s \approx +15^\circ\mathrm{C} \gg \mathcal{T}_e \approx -17^\circ\mathrm{C}$$

Impact of the greenhouse effect

*"Since solar radiation is mostly visible and near infrared, and Earth emits primarily thermal infrared radiation, the atmosphere may affect solar and terrestrial radiation very differently. [...] Since the atmospheric layer absorbs all of the energy emitted by the surface below it and emits like a **blackbody**, the only radiation emitted to space is from the atmosphere in this model." (Hartman, 2016, pages 32-32).*

Impact of the greenhouse effect

Figure 38: Zero-order model with greenhouse effect

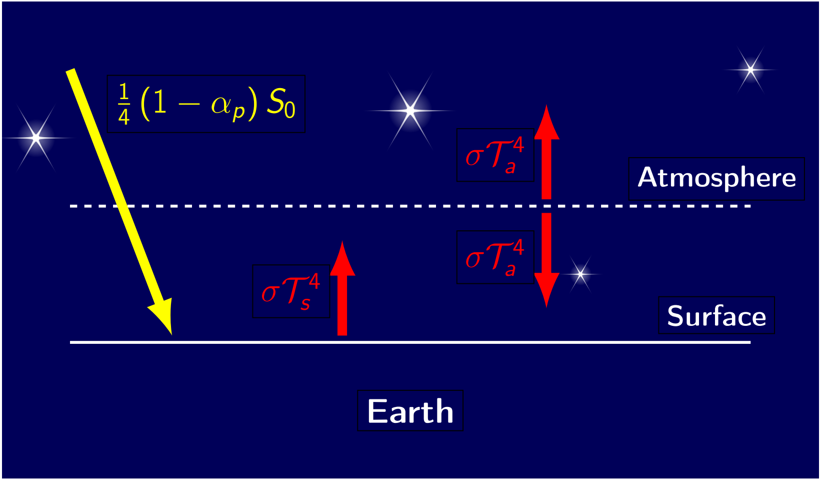

Impact of the greenhouse effect

- The energy balance for the Earth's surface is:

$$F_{\mathrm{solar}} + \sigma \mathcal{T}_{\mathrm{a}}^4 = \sigma \mathcal{T}_s^4$$

while the radiation balance for the atmosphere verifies:

$$\sigma \mathcal{T}_s^4 = 2\sigma \mathcal{T}_{\mathrm{a}}^4$$

- It follows that:

$$F_{\mathrm{solar}} + \sigma \mathcal{T}_{\mathrm{a}}^4 = 2\sigma \mathcal{T}_{\mathrm{a}}^4$$

or (we have $\sigma \mathcal{T}_e^4 = \frac{1}{4}\left(1-\alpha_p\right) S_0 := F_{\mathrm{solar}}$):

$$F_{\mathrm{solar}} = \sigma \mathcal{T}_{\mathrm{a}}^4 = \sigma \mathcal{T}_{\mathrm{e}}^4$$

- We conclude that:

$$\left\{\begin{array}{l} \mathcal{T}_{\mathrm{a}} = \mathcal{T}_{\mathrm{e}} \\ \mathcal{T}_s = \sqrt[4]{2}\,\mathcal{T}_{\mathrm{e}} \end{array}\right.$$

Impact of the greenhouse effect

- Using the previous numerical values, we obtain:

$$\left\{ \begin{array}{l} \mathcal{T}_{\mathrm{a}} = 255.81\,\mathrm{K} = -17.34^{\circ}\mathrm{C} \\ \mathcal{T}_{s} = 304.22\,\mathrm{K} = 31.07^{\circ}\mathrm{C} \end{array} \right.$$

- We find that the surface temperature is warmer than the observed global mean surface temperature
- **This is because the assumption that the atmosphere absorbs all the heat radiated from the surface is not true**

Impact of the greenhouse effect

- Another way to illustrate the greenhouse effect is to estimate the reflection parameter γ_p, which measures the net thermal radiation of the atmosphere with respect to the black body energy
- We deduce that the balance $\mathcal{E}_{\mathrm{net}}$ is:

$$\mathcal{E}_{\mathrm{net}} = F_{\mathrm{solar}} - \sigma \mathcal{T}_s^4 - \gamma_p \sigma \mathcal{T}_s^4$$

- Solving the equation $\mathcal{E}_{\mathrm{net}} = 0$ gives:

$$\gamma_p = 1 - \frac{F_{\mathrm{solar}}}{\sigma \mathcal{T}_s^4} = 1 - \frac{(1 - \alpha_p) S_0}{4 \sigma \mathcal{T}_s^4}$$

- Using a surface temperature of $15^\circ\mathrm{C}$, we get $\gamma_p = 0.3788$

$\Rightarrow$ Only 62% of the infrared radiation goes into space and 38% stays on the surface

Two-layer model of the atmosphere

"A layer of atmosphere that is almost opaque for longwave radiation can be crudely approximated as a blackbody that absorbs all terrestrial radiation that is incident upon it and emits like a blackbody at its temperature. For an atmosphere with a large infrared optical depth, the radiative transfer process can be represented with a series of blackbodies arranged in vertical layers. ***Two layers centered at 0.5 km and 2.0 km altitudes*** *provide a simple approximation for Earth's atmosphere." (Hartman, 2016, page 71).*

Two-layer model of the atmosphere

Figure 39: Two-layer model

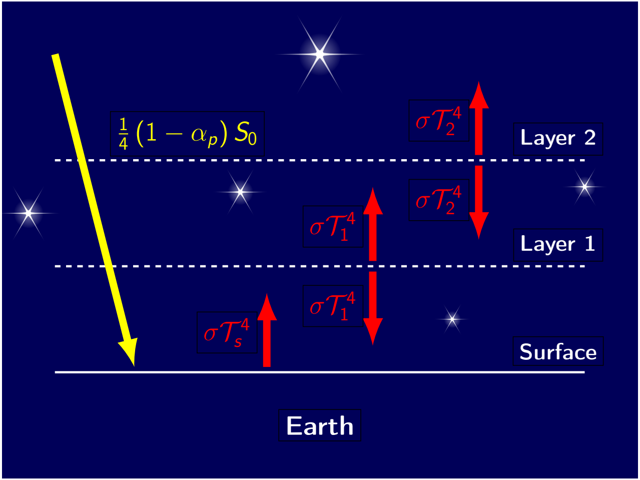

Two-layer model of the atmosphere

- We have:

$$\left\{\begin{array}{l} F_{\mathrm{solar}} + \sigma \mathcal{T}_1^4 = \sigma \mathcal{T}_s^4 \\ \sigma \mathcal{T}_2^4 + \sigma \mathcal{T}_s^4 = 2\sigma \mathcal{T}_1^4 \\ \sigma \mathcal{T}_1^4 = 2\sigma \mathcal{T}_2^4 \end{array}\right.$$

- By replacing F_{solar} by $\sigma \mathcal{T}_e^4$ and dividing the equations by σ, we get:

$$\left\{\begin{array}{l} \mathcal{T}_s^4 = 3\,\mathcal{T}_{\mathrm{e}}^4 \\ \mathcal{T}_1^4 = 2\,\mathcal{T}_{\mathrm{e}}^4 \\ \mathcal{T}_2^4 = 1\,\mathcal{T}_{\mathrm{e}}^4 \end{array}\right.$$

- The solution is then equal to:

$$\left\{\begin{array}{l} \mathcal{T}_s = \sqrt[4]{3}\,\mathcal{T}_{\mathrm{e}} = 336.67\,\mathrm{K} = 63.52^\circ\mathrm{C} \\ \mathcal{T}_1 = \sqrt[4]{2}\,\mathcal{T}_{\mathrm{e}} = 304.22\,\mathrm{K} = 31.07^\circ\mathrm{C} \\ \mathcal{T}_2 = \sqrt[4]{1}\,\mathcal{T}_{\mathrm{e}} = 255.81\,\mathrm{K} = -17.34^\circ\mathrm{C} \end{array}\right.$$

Multi-layer model of the atmosphere

- Let n be the total number of layers and $\mathcal{T}_k$ be the temperature at layer k
- We have:

$$\left\{ \begin{array}{l} \mathcal{T}_s = \mathcal{T}_0 = \sqrt[4]{n+1}\,\mathcal{T}_{\mathrm{e}} \\ \mathcal{T}_k = \sqrt[4]{n+1-k}\,\mathcal{T}_{\mathrm{e}} \qquad \text{for } k = 0, 1, \ldots, n \end{array} \right.$$

- The temperature decreases with the layer index:

$$\frac{\partial\,\mathcal{T}_k}{\partial\,k} = -\frac{1}{4}\,(n+1-k)^{-3/4}\,\mathcal{T}_{\mathrm{e}} \leq 0$$

Table 10: Layers of the Earth's atmosphere

Index	Layer	Altitude (in Km)
1	Troposphere	12
2	Stratosphere	50
3	Mesosphere	80
4	Thermosphere	500
5	Exosphere	6 200

Emissivity model of the atmosphere

Figure 40: One-layer model with atmospheric emissivity

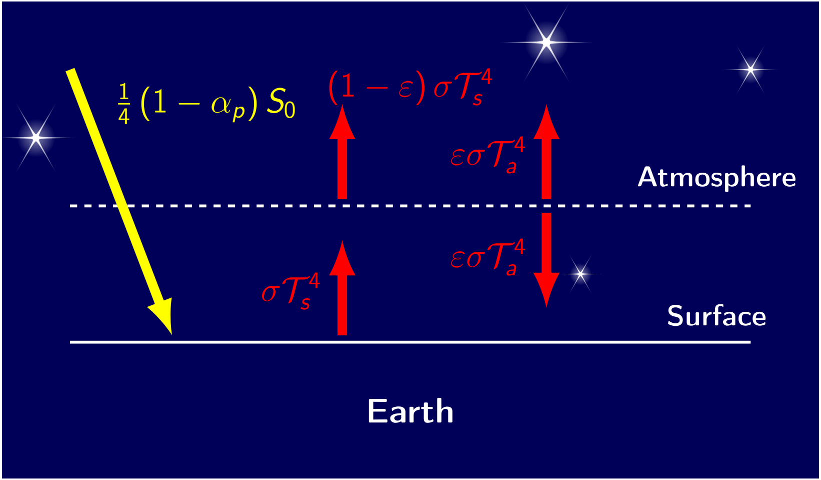

Emissivity model of the atmosphere

- The balance at the top of the atmosphere is:

$$F_{\mathrm{solar}} - (1 - \varepsilon)\,\sigma \mathcal{T}_s^4 - \varepsilon \sigma \mathcal{T}_a^4 = 0$$

- The balance of the atmosphere is:

$$\varepsilon \sigma \mathcal{T}_s^4 - 2\varepsilon \sigma \mathcal{T}_a^4 = 0$$

- The balance at the surface is:

$$F_{\mathrm{solar}} + \varepsilon \sigma \mathcal{T}_a^4 - \sigma \mathcal{T}_s^4 = 0$$

- The first equation is equivalent to:

$$(1 - \varepsilon)\,\sigma \mathcal{T}_s^4 + \varepsilon \sigma \mathcal{T}_a^4 = F_{\mathrm{solar}} = \sigma \mathcal{T}_e^4$$

- Using the second equation, it follows that:

$$\sigma \mathcal{T}_e^4 = (1 - \varepsilon)\,\sigma \mathcal{T}_s^4 + \frac{1}{2}\varepsilon \sigma \mathcal{T}_s^4 = \left(1 - \frac{1}{2}\varepsilon\right) \mathcal{T}_s^4$$

Emissivity model of the atmosphere

We conclude that:

$$\mathcal{T}_s = \sqrt[4]{\frac{2}{2-\varepsilon}}\mathcal{T}_e$$

and:

$$\mathcal{T}_a = \sqrt[4]{\frac{1}{2-\varepsilon}}\mathcal{T}_e$$

Therefore, for a given temperature $\mathcal{T}_s^\star$, we can find the unique value of the emissivity:

$$\varepsilon^\star = 2 - 2\left(\frac{\mathcal{T}_e}{\mathcal{T}_s^\star}\right)^4$$

Since $\mathcal{T}_s^\star \approx 15^\circ\mathrm{C}$, the emissivity of the atmosphere is 78%. This model then predicts an atmospheric temperature of $-30.8^\circ\mathrm{C}$

Emissivity model of the atmosphere

Figure 41: Relationship between atmospheric emissivity and temperature

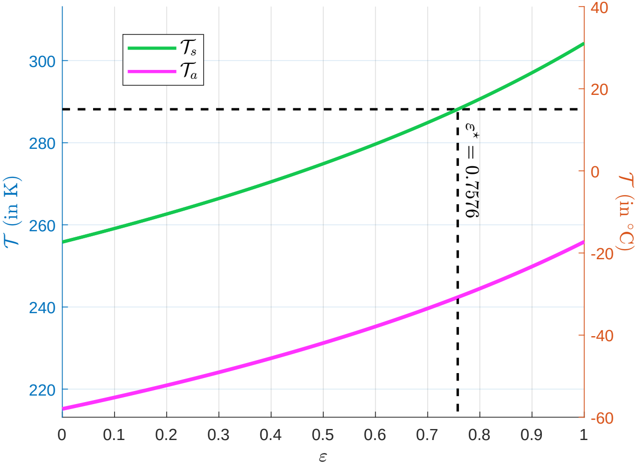

Emissivity model of the atmosphere

More generally, the Earth's energy balance is the sum of net shortwave radiation and net longwave radiation:

$$\mathcal{E}_{\mathrm{net}} = \underbrace{\mathcal{E}_{\mathrm{down}}^{\mathrm{short}} - \mathcal{E}_{\mathrm{up}}^{\mathrm{short}}}_{\text{Net shortwave}} + \underbrace{\mathcal{E}_{\mathrm{down}}^{\mathrm{long}} - \mathcal{E}_{\mathrm{up}}^{\mathrm{long}}}_{\text{Net longwave}}$$

where $\mathcal{E}_{\mathrm{down}}^{\mathrm{short/long}}$ is shortwave/longwave downward radiation and $\mathcal{E}_{\mathrm{up}}^{\mathrm{short/long}}$ is shortwave/longwave upward radiation

In the previous model, we have $\mathcal{E}_{\mathrm{net}}^{\mathrm{short}} = \frac{1}{4}(1 - \alpha_p) S_0$ and $\mathcal{E}_{\mathrm{net}}^{\mathrm{long}} = \varepsilon\sigma\mathcal{T}_a^4 - \sigma\mathcal{T}_s^4$

Emissivity model of the atmosphere

Figure 42: Earth's Energy Budget

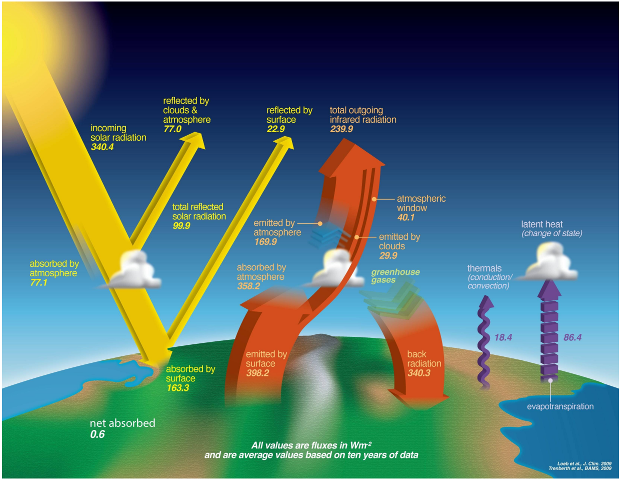

Specific heat capacity

Definition

The specific heat capacity c of a substance is the heat capacity C of the substance divided by the mass of the substance:

$$c = \frac{C}{M} = \frac{1}{M} \frac{\Delta \mathcal{E}}{\Delta \mathcal{T}} \tag{1}$$

where:

- $\Delta \mathcal{E}$ is the amount of heat required to raise the temperature of the substance by $\Delta \mathcal{T}$
- M is the mass of the substance in kilograms (kg)
- $\Delta \mathcal{E}$ is the change in energy in joules (J)
- $\Delta \mathcal{T}$ is the change in temperature in Kelvin (K)
- c is the specific heat capacity in joules per kilogram per Kelvin $(\mathrm{J\,kg^{-1}\,K^{-1}})$

Specific heat capacity

- The specific heat capacity of water is $4\,186\,\mathrm{J\,kg^{-1}\,K^{-1}}$
- From Equation (1), we deduce that:

$$\Delta\mathcal{E} = Mc\,\Delta\mathcal{T} \tag{2}$$

- In this case, the amount of energy required to raise the temperature of $1\,\mathrm{m}^3$ of water by $10^\circ\mathrm{C}$ is equal to:

$$\Delta\mathcal{E} = 10^3 \times 4\,186 \times 10 = 4\,186\,000\,\mathrm{J}$$

Specific heat capacity

- The specific heat capacity of air is about $1\,000\,\mathrm{J\,kg^{-1}\,K^{-1}}$
- The mass of the atmosphere is $5.148 \times 10^{18}\,\mathrm{kg}$
- The amount of energy required to raise the temperature of the atmosphere by $1^\circ\mathrm{C}$ is:

$$\begin{aligned}\Delta\mathcal{E} &= \left(5.148 \times 10^{18}\,\mathrm{kg}\right) \times \left(1\,000\,\mathrm{J\,kg^{-1}\,K^{-1}}\right) \times 1\,\mathrm{K} \\ &= 5.148 \times 10^{21}\,\mathrm{J}\end{aligned}$$

Specific heat capacity

- We can write Equation (1) as follows:

$$\Delta \mathcal{T} = \frac{\Delta \mathcal{E}}{Mc} \tag{3}$$

- This equation gives the change in temperature for a change in energy. For example, adding 1 000 joules of energy to one liter of water will increase its temperature by about $0.239^{\circ}\mathrm{C}$:

$$\Delta \mathcal{T} = \frac{1000}{1 \times 4\,186} = 0.239$$

Specific heat capacity

- Equations (1)–(3) can be modified by scaling the mass M of the substance to standardize the required energy $\Delta\mathcal{E}$
- A possible scaling factor can be the surface area:

$$m = \frac{M}{\mathcal{A}rea}$$

and we get:

$$\Delta\mathcal{E} = mc\,\Delta\mathcal{T} \tag{4}$$

- For the atmosphere, we have:

$$m = \frac{M}{\mathcal{A}rea} = \frac{5.148 \times 10^{18}\,\mathrm{kg}}{510.0645 \times 10^{6} \times 10^{6}\,\mathrm{m}^2} = 1.0093 \times 10^{4}\,\mathrm{kg}\,\mathrm{m}^{-2}$$

because the radius r of the Earth is $6\,371\,\mathrm{km}$ and the surface of the Earth is approximately $\mathcal{A}rea = 4\pi r^2 = 510.0645$ million km^2

Specific heat capacity

- In some climate modeling textbooks, Equation (4) is expressed using other formulas for the mass of the atmosphere per unit area
- For example, m can be replaced by the product of height h and density ρ, or by the ratio of pressure p to gravitational acceleration g. However, all these quantities are equivalent because we have:

$$m = h\rho = \left(8.2 \times 10^3 \,\mathrm{m}\right) \times \left(1.225 \,\mathrm{kg}\,\mathrm{m}^{-3}\right) = 1.0045 \times 10^3 \,\mathrm{kg}\,\mathrm{m}^{-2}$$

and:

$$m = \frac{p}{g} = \frac{101\,325 \,\mathrm{Pa}}{9.81 \,\mathrm{m}\,\mathrm{s}^{-2}} = \frac{101\,325 \,\mathrm{m}^{-1}\,\mathrm{kg}\,\mathrm{s}^{-2}}{9.81 \,\mathrm{m}\,\mathrm{s}^{-2}} = 1.0329 \times 10^4 \,\mathrm{kg}\,\mathrm{m}^{-2}$$

where $h = 8.2 \,\mathrm{km}$ is the height of the atmosphere, $\rho = 1.225 \,\mathrm{kg}\,\mathrm{m}^{-3}$ is the density of the atmosphere, $p = 101\,325 \,\mathrm{Pa}$ is the standard atmospheric pressure at sea level on Earth, and $g = 9.81 \,\mathrm{m}\,\mathrm{s}^{-2}$ is the acceleration due to gravity at the Earth's surface
- Therefore, we obtain the following equivalent formulas:

$$mc\,\Delta\mathcal{T} = h\rho c\,\Delta\mathcal{T} = \frac{p}{g}c\,\Delta\mathcal{T} = \Delta\mathcal{E}$$

Radiative relaxation timescale

- We transform Equation (4) into a differential equation:

$$mc\frac{\mathrm{d}\mathcal{T}}{\mathrm{d}t} = \frac{\mathrm{d}\boldsymbol{\mathcal{E}}}{\mathrm{d}t}$$

- For a black body, we have:

$$F_{\mathrm{solar}} - \sigma\mathcal{T}^4 = 0$$

- We deduce that:

$$\begin{aligned} \boldsymbol{\mathcal{E}} &= F_{\mathrm{solar}} - \sigma\mathcal{T}^4 \\ &= \sigma\mathcal{T}_e^4 - \sigma\mathcal{T}^4 \end{aligned}$$

Radiative relaxation timescale

- Let us assume that $\mathcal{T} = \mathcal{T}_e + \Delta\mathcal{T}$. It follows that:

$$mc \frac{\mathrm{d}\Delta\mathcal{T}}{\mathrm{d}t} = -4\sigma\mathcal{T}_e^3 \Delta\mathcal{T}$$

because:

$$\frac{\partial}{\partial \Delta\mathcal{T}} \left(\sigma\mathcal{T}_e^4 - \sigma\mathcal{T}^4\right) = -4\sigma\mathcal{T}_e^3$$

- Let τ_e be the radiative relaxation timescale defined as:

$$\tau_e = \frac{mc}{4\sigma\mathcal{T}_e^3}$$

- We have:

$$\left\{ \begin{array}{l} \dfrac{\mathrm{d}\Delta\mathcal{T}}{\mathrm{d}t} = -\dfrac{1}{\tau_e}\Delta\mathcal{T} \\ \Delta\mathcal{T}(0) = \Delta\mathcal{T}_0 \end{array} \right.$$

Radiative relaxation timescale

- The solution of this ordinary differential equation is well-known and we get:

$$\Delta\mathcal{T}(t) = \exp\left(-\frac{t}{\tau_e}\right)\Delta\mathcal{T}_0$$

- $\Delta\mathcal{T}(t)$ gives the impulse response of an initial temperature shock of $\Delta\mathcal{T}_0$
- Because $\tau_e > 0$, we conclude that the system is stable:

$$\lim_{t\to\infty}\Delta\mathcal{T}(t) = 0$$

- We note that the equation for $\Delta\mathcal{T}(t)$ describes an exponential survival function with parameter τ_e^{-1}
- We deduce that the radiative relaxation timescale τ_e is the mean lifetime

Radiative relaxation timescale

Numerical value of τ_e

Using the previously obtained values for the atmosphere ($m = 1.0093 \times 10^4 \,\mathrm{kg\,m^{-2}}$, $c = 1\,000 \,\mathrm{J\,kg^{-1}\,K^{-1}}$ and $\mathcal{T}_e = 255.81 \,\mathrm{K}$), the radiative relaxation timescale is equal to 31 days:

$$
\begin{aligned}
\tau_e &= \frac{\left(1.0093 \times 10^4 \,\mathrm{kg\,m^{-2}}\right) \times \left(1\,000 \,\mathrm{J\,kg^{-1}\,K^{-1}}\right)}{4 \times \left(5.67 \times 10^{-8} \,\mathrm{W\,m^{-2}\,K^{-4}}\right) \times \left(255.81 \,\mathrm{K}\right)^3} \\
&= 2\,658\,427 \,\mathrm{J\,W^{-1}} \\
&= \frac{2\,658\,427 \,\mathrm{s}}{24 \times 3\,600 \,\mathrm{s}} \\
&= 30.77 \,\mathrm{days}
\end{aligned}
$$

Radiative relaxation timescale

Figure 43: Impulse response function for $\Delta\mathcal{T}_0 = +1^\circ\mathrm{C}$ and a black body

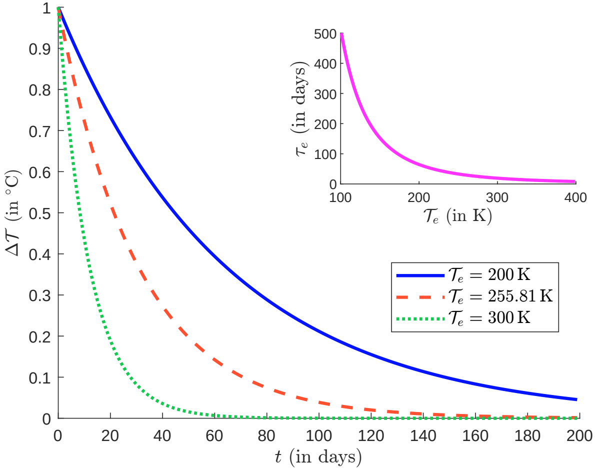

Radiative relaxation timescale

- For a gray body, we found that:

$$\sigma \mathcal{T}_e^4 = (2-\varepsilon)\,\sigma \mathcal{T}_a^4 = \left(\frac{2-\varepsilon}{2}\right)\sigma \mathcal{T}_s^4$$

- We deduce that:

$$mc\frac{\mathrm{d}\mathcal{T}_a}{\mathrm{d}t} = \frac{\mathrm{d}}{\mathrm{d}t}\left(\sigma \mathcal{T}_e^4 - (2-\varepsilon)\,\sigma \mathcal{T}_a^4\right)$$

and:

$$mc\frac{\mathrm{d}\mathcal{T}_s}{\mathrm{d}t} = \frac{\mathrm{d}}{\mathrm{d}t}\left(\sigma \mathcal{T}_e^4 - \left(\frac{2-\varepsilon}{2}\right)\sigma \mathcal{T}_s^4\right)$$

- We obtain:

$$\Delta \mathcal{T}_a(t) = \exp\left(-\frac{t}{\tau_a}\right)\Delta \mathcal{T}_0 \quad \text{and} \quad \Delta \mathcal{T}_s(t) = \exp\left(-\frac{t}{\tau_s}\right)\Delta \mathcal{T}_0$$

where:

$$\tau_a = \frac{mc}{4\,(2-\varepsilon)\,\sigma \mathcal{T}_e^3} \quad \text{and} \quad \tau_s = \frac{mc}{2\,(2-\varepsilon)\,\sigma \mathcal{T}_e^3}$$

Radiative relaxation timescale

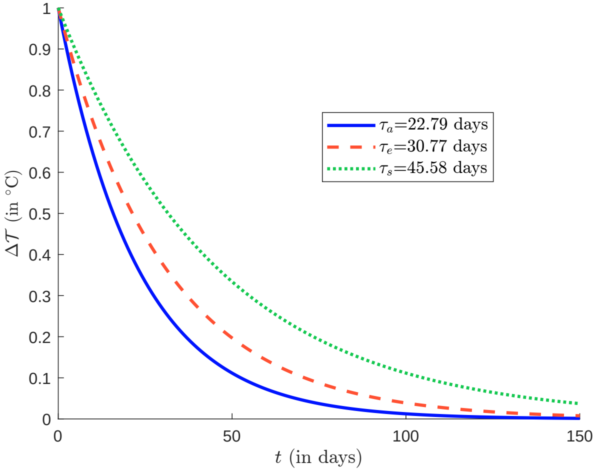

Figure 44: Impulse response function for $\Delta\mathcal{T}_0 = +1^\circ\mathrm{C}$ and a gray body[5]

[5]We consider an emissivity value of 65%

Mathematical definition of climate sensitivity and feedback

"[...] Climate forcing is a change to the climate system that can be expected to change the climate. Examples would be doubling the CO_2, increasing the total solar irradiance (TSI) by 2%, introducing volcanic aerosols into the stratosphere, etc. Climate forcings are usually quantified in terms of how many $\mathrm{W/m^2}$ *they change the energy balance when imposed. For example, instantaneously doubling the CO_2 changes the energy balance at the top of the atmosphere by about* $4\,\mathrm{W/m^2}$*. A feedback process is a response of the climate system to surface warming that then alters the energy balance in such a way as to change the temperature response to the forcing. A* ***positive feedback*** *makes the forced response bigger, and a* ***negative feedback*** *makes it smaller. Classic examples of positive feedbacks are ice-albedo feedback and water-vapor feedback. When it warms, ice melts, and this reduces Earth's albedo and causes further warming. When it cools, ice grows, and this increases Earth's albedo, causing further cooling [...]." Hartmann (2016, page 294).*

Mathematical definition of climate sensitivity and feedback

- We assume that some extra energy ΔF is added to the system
- ΔF is called the radiative forcing and is measured in W/m^2
- The climate response is generally measured as the change in the surface temperature $\Delta \mathcal{T}_s$

Definition of the climate sensitivity

The climate sensitivity is defined as:

$$\phi := \frac{\Delta \mathcal{T}_s}{\Delta F}$$

Using differential notation, we have:

$$\phi := \frac{\mathrm{d}\mathcal{T}_s}{\mathrm{d}F}$$

implying that:

$$\mathrm{d}\mathcal{T}_s = \phi \, \mathrm{d}F$$

Mathematical definition of climate sensitivity and feedback

Feedback mechanism

- We assume that the perturbation $\mathrm{d}F$ depends on the temperature $\mathcal{T}_s$ and some exogenous factors x_i:

$$\mathrm{d}F = \frac{\partial F}{\partial \mathcal{T}_s}\mathrm{d}\mathcal{T}_s + \sum_{i=1}^{n} \frac{\partial F}{\partial x_i}\mathrm{d}x_i$$

- We conclude that:

$$\left(1 - \phi \frac{\partial F}{\partial \mathcal{T}_s}\right)\mathrm{d}\mathcal{T}_s = \phi \sum_{i=1}^{n} \frac{\partial F}{\partial x_i}\mathrm{d}x_i$$

- We then get a feedback mechanism, because the temperature dynamics depend on the factors x_i, but also on the temperature response

Climate feedback

- For the one-layer model with emissivity, we have $\mathcal{E} = 0$ where:

$$\begin{aligned}\mathcal{E} &= F_{\mathrm{solar}} - \left(\frac{2-\varepsilon}{2}\right)\sigma\mathcal{T}_s^4 \\ &= \frac{1}{4}\left(1-\alpha_p\right)S_0 - \left(\frac{2-\varepsilon}{2}\right)\sigma\mathcal{T}_s^4\end{aligned}$$

- The first-order Taylor Series expansion of $\mathcal{E} = 0$ gives:

$$\Delta\mathcal{E} = \frac{1}{4}\left(1-\alpha_p\right)\Delta S_0 - \frac{1}{4}S_0\Delta\alpha_p + \frac{1}{2}\sigma\mathcal{T}_s^4\Delta\varepsilon - 4\left(\frac{2-\varepsilon}{2}\right)\sigma\mathcal{T}_s^3\Delta\mathcal{T}_s$$

- Remember that each perturbation Δy depends on the temperature $\mathcal{T}_s$ and some exogenous factors x_i:

$$\Delta y = \frac{\partial y}{\partial\mathcal{T}_s}\Delta\mathcal{T}_s + \sum_{i=1}^{n}\frac{\partial y}{\partial x_i}\Delta x_i$$

Climate feedback

- We have:

$$\begin{aligned}\Delta\mathcal{E} &= \frac{1}{4}\left(1-\alpha_p\right)\Delta S_0 - \frac{1}{4}S_0\left(\frac{\partial\alpha_p}{\partial\mathcal{T}_s}\Delta\mathcal{T}_s + \sum_{i=1}^{n}\frac{\partial\alpha_p}{\partial x_i}\Delta x_i\right) + \\ &\quad \frac{1}{2}\sigma\mathcal{T}_s^4\left(\frac{\partial\varepsilon}{\partial\mathcal{T}_s}\Delta\mathcal{T}_s + \sum_{i=1}^{n}\frac{\partial\varepsilon}{\partial x_i}\Delta x_i\right) - 4\left(\frac{2-\varepsilon}{2}\right)\sigma\mathcal{T}_s^3\Delta\mathcal{T}_s\end{aligned}$$

- We deduce that:

$$\Delta\mathcal{E} = \lambda\Delta\mathcal{T}_s + \sum_{i=0}^{n}\Delta F_i$$

where $\Delta F_0 := \Delta F_{\mathrm{solar}} = \frac{1}{4}\left(1-\alpha_p\right)\Delta S_0$,

$$\Delta F_i = \left(-\frac{1}{4}S_0\frac{\partial\alpha_p}{\partial x_i} + \frac{1}{2}\sigma\mathcal{T}_s^4\frac{\partial\varepsilon}{\partial x_i}\right)\Delta x_i \qquad \text{for } i \geq 1$$

$$\lambda = -\frac{1}{4}S_0\frac{\partial\alpha_p}{\partial\mathcal{T}_s} + \frac{1}{2}\sigma\mathcal{T}_s^4\frac{\partial\varepsilon}{\partial\mathcal{T}_s} - 4\left(\frac{2-\varepsilon}{2}\right)\sigma\mathcal{T}_s^3$$

Climate feedback

- Since $\Delta\mathcal{E}$ and ΔF_i are measured in $\mathrm{W/m^2}$ and $\Delta\mathcal{T}_s$ is measured in Kelvin, we deduce that λ is measured in $\mathrm{W\,m^{-2}\,K^{-1}}$
- We transform $\Delta\mathcal{E}$ into $\Delta\mathcal{T}_s$ by considering the heat capacity c expressed in $\mathrm{W\,m^{-2}\,K^{-1}\,s}$:

$$c\frac{\mathrm{d}\Delta\mathcal{T}_s}{\mathrm{d}t} = \lambda\Delta\mathcal{T}_s + \Delta F \tag{5}$$

  where $\Delta F = \sum_{i=0}^{n} F_i$
- **The climate feedback parameter λ can be positive or negative**, and we have the following mathematical properties:
  - If $\lambda > 0$, the system is unstable;
  - If $\lambda < 0$, the system is stable and the equilibrium is reached when:

$$\Delta\mathcal{T}_s = \Delta\mathcal{T}_s^{\star} = -\frac{\Delta F}{\lambda} = -\phi\Delta F \tag{6}$$

Climate feedback

- We see that the climate feedback parameter can be decomposed into three components:

$$\lambda = \lambda_0 + \lambda_{\alpha_p} + \lambda_\varepsilon$$

where:

1. λ_0 is the Planck feedback or the black body response:

$$\lambda_0 = -4 \left(\frac{2 - \varepsilon}{2} \right) \sigma \mathcal{T}_s^3$$

2. λ_{α_p} is the surface albedo feedback:

$$\lambda_{\alpha_p} = -\frac{1}{4} S_0 \frac{\partial \alpha_p}{\partial \mathcal{T}_s}$$

3. λ_ε is the emissivity feedback:

$$\lambda_\varepsilon = \frac{1}{2} \sigma \mathcal{T}_s^4 \frac{\partial \varepsilon}{\partial \mathcal{T}_s}$$

Planck feedback

Since $\varepsilon < 1$, the Planck feedback is negative, meaning that it stabilizes the climate and counteracts global warming. In fact, as the Earth warms, it emits more thermal radiation into space, and this increased longwave radiation acts as a natural cooling mechanism. Conversely, as the Earth cools, it emits less thermal radiation into space, and this decreased longwave radiation acts as a natural warming mechanism

Earlier we found that $\varepsilon = 0.78$. So the estimate of λ_0 is[6]:

$$\begin{aligned}\lambda_0 &= -4\left(\frac{2-0.78}{2}\right) \times \left(5.67 \times 10^{-8}\right) \times (273.15+15)^3 \\ &= -3.310\,\mathrm{W\,m^{-2}\,K^{-1}}\end{aligned}$$

[6] For comparison, the most recent estimate is $-3.22\,\mathrm{W\,m^{-2}\,K^{-1}}$, while the 90% confidence interval is from -3.4 to $-3.0\,\mathrm{W\,m^{-2}\,K^{-1}}$ (IPCC, 2021, Chapter 7, page 968)

Albedo feedback

- The sign of the surface albedo feedback depends on the sign of $\dfrac{\partial \alpha_p}{\partial \mathcal{T}_s}$
- Two main factors play a role in determining α_p:

> *"The albedo of the planet for solar radiation is primarily determined by the clouds and surface, with the main variable component of the latter being the ice/snow cover." (Hansen et al., 1984, page 166).*

- If the Earth were completely covered in ice, its albedo α_p would be about 84%, meaning it would reflect most of the sunlight that hits it
- If the Earth were covered by a dark green forest canopy, the albedo would be about 14%
- Cloud albedo feedback occurs because changes in cloud cover, cloud altitude or cloud properties affect the amount of reflected shortwave radiation. This feedback can be either positive or negative

Albedo feedback

- According to IPCC AR6, the value of the global surface albedo feedback is estimated to be $0.35\,\mathrm{W\,m^{-2}\,K^{-1}}$, with a 90% confidence interval from 0.10 to $0.60\,\mathrm{W\,m^{-2}\,K^{-1}}$
- This means that:

$$\frac{\partial \alpha_p}{\partial \mathcal{T}_s} = -\frac{4\lambda_{\alpha_p}}{\mathcal{S}_0} = -\frac{4 \times 0.35}{1368} = -1.023 \times 10^{-3}$$

Ice-albedo feedback modeling (Sellers model)

- If $\alpha_p = f_{\mathrm{albedo}}(\mathcal{T}_s)$, then $\lambda_{\alpha_p} = -\frac{1}{4} S_0 f'_{\mathrm{albedo}}(\mathcal{T}_s)$
- Sellers (1969) suggested:

$$\alpha_p = \begin{cases} b(\phi) - 0.009\mathcal{T}_s & \text{if } \mathcal{T}_s \leq 283.16\,\mathrm{K} \\ b(\phi) - 2.548 & \text{if } \mathcal{T}_s \geq 283.16\,\mathrm{K} \end{cases}$$

  where $b(\phi)$ is an estimated coefficient that depends on the latitude ϕ
- On average we have $\overline{b(\phi)} = 2.8811$
- We deduce that:

$$\lambda_{\alpha_p} = \frac{1}{4} \times 1\,368 \times 0.009 = 3.078\,\mathrm{W\,m^{-2}\,K^{-1}}$$

- It is obvious that this positive feedback has been overestimated. The reason is that snow and sea ice cover about 10% of the Earth's surface. Therefore, we get $\lambda_{\alpha_p} \approx 0.3\,\mathrm{W\,m^{-2}\,K^{-1}}$

Ice-albedo feedback modeling (Sellers model)

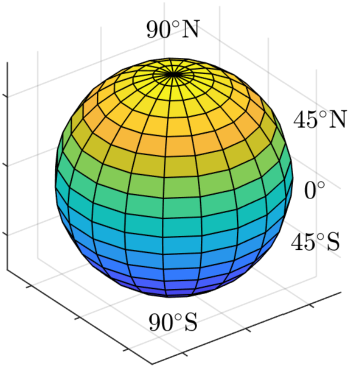

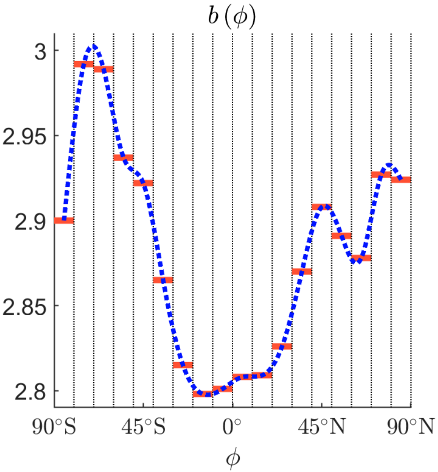

Ice-albedo feedback modeling (Budyko model)

- Budyko (1969) assumed that:

$$\alpha_p = \begin{cases} \alpha_{\mathrm{cold}} & \text{if } \mathcal{T}_s \leq \mathcal{T}_{\mathrm{cold}} \\ \alpha_{\mathrm{warm}} + (\alpha_{\mathrm{cold}} - \alpha_{\mathrm{warm}}) \left(\dfrac{\mathcal{T}_{\mathrm{warm}} - \mathcal{T}_s}{\mathcal{T}_{\mathrm{warm}} - \mathcal{T}_{\mathrm{cold}}} \right)^{\eta} & \text{if } \mathcal{T}_{\mathrm{cold}} \leq \mathcal{T}_s \leq \mathcal{T}_{\mathrm{warm}} \\ \alpha_{\mathrm{warm}} & \text{if } \mathcal{T}_s \geq \mathcal{T}_{\mathrm{warm}} \end{cases}$$

  where $\eta \geq 1$
- It follows that:

$$\lambda_{\alpha_p}(\mathcal{T}_s) = \frac{1}{4}\eta S_0 (\alpha_{\mathrm{cold}} - \alpha_{\mathrm{warm}}) \frac{(\mathcal{T}_{\mathrm{warm}} - \mathcal{T}_s)^{\eta-1}}{(\mathcal{T}_{\mathrm{warm}} - \mathcal{T}_{\mathrm{cold}})^{\eta}} \cdot \mathbb{1}\left\{\mathcal{T}_{\mathrm{cold}} \leq \mathcal{T}_s \leq \mathcal{T}_{\mathrm{warm}}\right\}$$

- Using the values $\alpha_{\mathrm{cold}} = 0.7$, $\mathcal{T}_{\mathrm{cold}} = 260\,\mathrm{K}$, $\alpha_{\mathrm{warm}} = 0.3$, $\mathcal{T}_{\mathrm{warm}} = 295\,\mathrm{K}$ and $\eta = 2$, we get $\lambda_{\alpha_p}(282\,\mathrm{K}) = 2.90\,\mathrm{W\,m^{-2}\,K^{-1}}$, $\lambda_{\alpha_p}(288\,\mathrm{K}) = 1.56\,\mathrm{W\,m^{-2}\,K^{-1}}$ and $\lambda_{\alpha_p}(293\,\mathrm{K}) = 0.45\,\mathrm{W\,m^{-2}\,K^{-1}}$

Emissivity feedback

- The emissivity feedback is the sum of several components:

$$\lambda_{\varepsilon} = \lambda_{\text{water vapor}} + \lambda_{\text{lapse rate}} + \lambda_{\text{cloud longwave}} + \cdots$$

Emissivity feedback (water vapor)

- The **water vapor feedback**, also known as the specific humidity feedback, is the most important positive and destabilizing feedback. It can be described as follows:

  > *"[...] As the temperature increases, the amount of water vapor in saturated air increases. Since water vapor is the principal greenhouse gas, increasing water vapor content will increase the greenhouse effect of the atmosphere and raise the surface temperature even further." (Hartmann, 2016, page 297).*

- According to IPCC AR6, the value $\lambda_{\text{water vapor}}$ of the water vapor feedback is assessed to be $1.85\,\mathrm{W}\,\mathrm{m}^{-2}\,\mathrm{K}^{-1}$

Emissivity feedback (lapse rate)

- The **lapse rate mechanism** describes the relationship between temperature and altitude in the atmosphere:

$$\Gamma = -\frac{\partial \mathcal{T}}{\partial z} \in \left[4\,\mathrm{K\,km^{-1}}, 10\,\mathrm{K\,km^{-1}}\right]$$

  where z is the altitude in kilometers

- On average, the lapse rate is about $6.5°\mathrm{C}$ per kilometer
- According to IPCC AR6, the average value of $\lambda_{\text{lapse rate}}$ is $-0.50\,\mathrm{W\,m^{-2}\,K^{-1}}$

Emissivity feedback (clouds)

- The case of **cloud feedbacks** is more complicated because it involves several mechanisms:
  1. high cloud altitude
  2. tropical high cloud amount
  3. subtropical marine low cloud
  4. land cloud
  5. midlatitude cloud amount
  6. extratropical cloud optical depth
  7. Arctic cloud
- According to IPCC AR6, the value λ_{cloud} of the net cloud feedback is estimated to be $0.42\,\mathrm{W\,m^{-2}\,K^{-1}}$
- One of the difficulties is to decompose the cloud feedback into shortwave and longwave feedbacks, since the global surface albedo feedback already includes shortwave cloud mechanisms. Assuming that $2/3$ of the cloud feedback is longwave radiation, we get:

$$\lambda_{\varepsilon} \approx 1.85 - 0.50 + \frac{2}{3} \times 0.42 = 1.63\,\mathrm{W\,m^{-2}\,K^{-1}}$$

Total feedback (deterministic analysis)

- We have:

$$\begin{aligned}\lambda &= \lambda_0 + \lambda_{\alpha_p} + \lambda_\varepsilon \\ &= -3.31 + 0.35 + 1.63 \\ &= -1.33\,\mathrm{W\,m^{-2}\,K^{-1}}\end{aligned}$$

- This value is obtained with a simple one-layer model with emissivity

Total feedback (stochastic analysis)

- We assume that $\tilde{\lambda} \sim \mathcal{N}\left(\mu_\lambda, \sigma_\lambda^2\right)$
- As before, we decompose the feedback as a sum of individual feedbacks:

$$\tilde{\lambda} = \sum_{i=1}^{n} \tilde{\lambda}_i$$

where $\tilde{\lambda}_i \sim \mathcal{N}\left(\mu_i, \sigma_i^2\right)$

- Assuming that the individual feedbacks are independent, we have:

$$\left\{ \begin{array}{l} \mu_\lambda = \sum_{i=1}^{n} \mu_i \\ \sigma_\lambda = \sqrt{\sum_{i=1}^{n} \sigma_i^2} \end{array} \right.$$

Total feedback (stochastic analysis)

Table 11: Parameters μ_i and σ_i of feedback parameters

Feedback mechanism	μ_i	σ_i	Shortwave
High-cloud altitude	+0.20	0.10	
Tropical marine low cloud	+0.25	0.16	
Tropical anvil cloud area	−0.20	0.20	
Land cloud amount	+0.08	0.08	
Middle-latitude marine low-cloud amount	+0.12	0.12	
High-latitude low-cloud optical depth	+0.00	0.10	✓
Planck feedback	−3.20	0.10	✓
Water vapor + lapse rate	+1.15	0.15	
Surface albedo	+0.30	0.15	✓
Total cloud	+0.45	0.33	
Stratospheric	+0.00	0.10	
Atmospheric composition changes	+0.00	0.15	
Climate feedback parameter	−1.30	0.44	

Source: Sherwood *et al.* (2020, Table 1, page 18).

Total feedback (cloud feedback)

Figure 45: Probability density function of individual cloud feedbacks

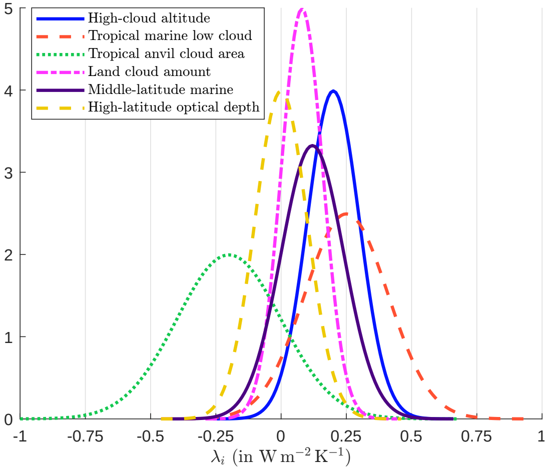

Total feedback (cloud feedback)

Using the parameters of the individual cloud feedbacks, the distribution of the total cloud feedback is Gaussian with:

$$\begin{aligned}\mu_{\text{total cloud}} &= 0.20 + 0.25 - 0.20 + 0.08 + 0.12 + 0.00 \\ &= 0.45\,\mathrm{W\,m^{-2}\,K^{-1}}\end{aligned}$$

and:

$$\begin{aligned}\sigma_{\text{total cloud}} &= \sqrt{0.10^2 + 0.16^2 + 0.20^2 + 0.08^2 + 0.12^2 + 0.10^2} \\ &= 0.3262\,\mathrm{W\,m^{-2}\,K^{-1}}\end{aligned}$$

Total feedback (positive feedback)

Figure 46: Probability density function of positive feedbacks

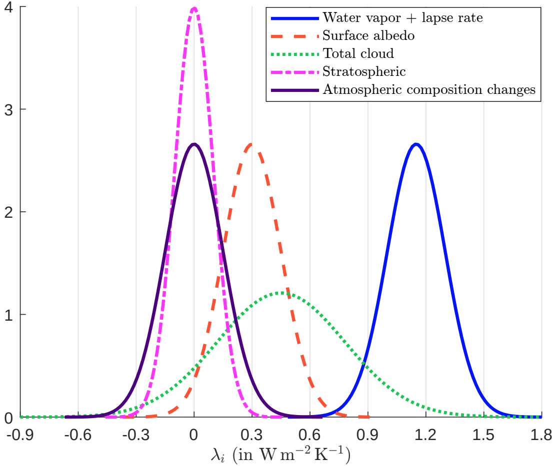

Total feedback (positive feedback)

The aggregate positive feedback is the sum of the five main positive feedback components:

$$\mu_{\text{positive}} = 1.15 + 0.30 + 0.45 + 0.00 + 0.00 = 1.90\,\mathrm{W\,m^{-2}\,K^{-1}}$$

and:

$$\sigma_{\text{positive}} = \sqrt{0.15^2 + 0.15^2 + 0.33^2 + 0.10^2 + 0.15^2} = 0.4317\,\mathrm{W\,m^{-2}\,K^{-1}}$$

Total feedback

Figure 47: Comparison of $\tilde{\lambda}_{\text{Planck}}$ and $\tilde{\lambda}_{\text{positive}}$

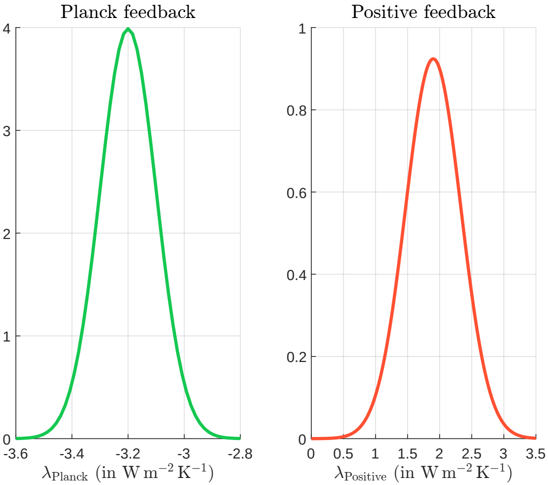

Total feedback

- If we aggregate the positive feedback with the Planck feedback, the climate feedback parameter is $\tilde{\lambda} \sim \mathcal{N}\left(\mu_\lambda, \sigma_\lambda^2\right)$ where:

$$\begin{aligned}\mu_\lambda &= -1.30\,\mathrm{W\,m^{-2}\,K^{-1}} \\ \sigma_\lambda &= 0.44\,\mathrm{W\,m^{-2}\,K^{-1}}\end{aligned}$$

- The probability that the climate feedback is positive is small:

$$\begin{aligned}\Pr\left\{\tilde{\lambda} \geq 0\right\} &= \Pr\left\{\frac{\tilde{\lambda} - \mu_\lambda}{\sigma_\lambda} \geq -\frac{\mu_\lambda}{\sigma_\lambda}\right\} \\ &= 1 - \Phi\left(-\frac{\mu_\lambda}{\sigma_\lambda}\right) \\ &= 1 - \Phi\left(\frac{1.30}{0.44}\right) \\ &= 0.16\%\end{aligned}$$

Total feedback

Figure 48: Probability density function of the climate feedback parameter

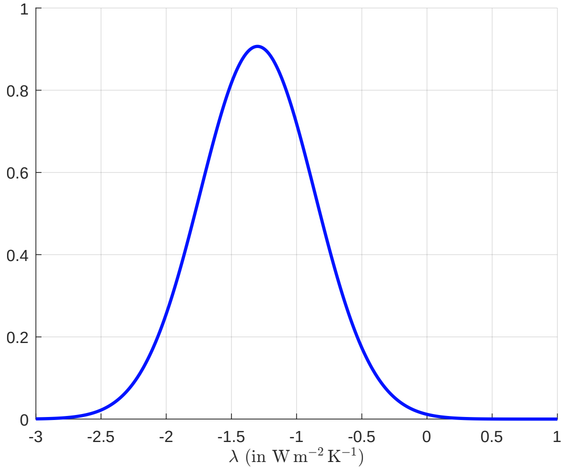

Equilibrium climate sensitivity (ECS)

Definition of ECS

We recall that the definition of equilibrium is:

$$\Delta \mathcal{T}_s^\star = -\frac{\Delta F}{\lambda} = -\phi \Delta F$$

Earth's **equilibrium climate sensitivity** (ECS) is the long-term global mean surface temperature change due to a specific value of radiative forcing corresponding to a doubling of CO_2 in the atmosphere:

$$\mathrm{ECS} := \Delta \mathcal{T}_{2 \times \mathrm{CO}_2} = -\frac{\Delta F_{2 \times \mathrm{CO}_2}}{\lambda}$$

where ECS (or $\Delta \mathcal{T}_{2 \times \mathrm{CO}_2}$) is the equilibrium climate sensitivity, λ is the climate sensitivity parameter and $\Delta F_{2 \times \mathrm{CO}_2}$ is the radiative forcing resulting from a doubling of the atmospheric carbon dioxide concentration

Stochastic equilibrium temperature modeling

- We assume $\Delta F = 4\,\mathrm{W/m^2}$ and $\lambda = -1.33\,\mathrm{W\,m^{-2}\,K^{-1}}$
- The equilibrium warming is then equal to $3^\circ\mathrm{C}$:

$$\Delta \mathcal{T}_s^\star = -\frac{4\,\mathrm{W/m^2}}{-1.33\,\mathrm{W\,m^{-2}\,K^{-1}}} = 3.0075\,\mathrm{K}$$

- Remember that the dynamics of the temperature change is given by the ordinary differential equation:

$$c\frac{\mathrm{d}\Delta \mathcal{T}_s}{\mathrm{d}t} = \lambda \Delta \mathcal{T}_s + \Delta F$$

- We assume that the solution has the following form:

$$\Delta \mathcal{T}_s(t) = e^{At}B + C$$

- We deduce that:

$$\frac{\mathrm{d}\Delta \mathcal{T}_s}{\mathrm{d}t} = Ae^{At}B = A\left(\Delta \mathcal{T}_s(t) - C\right)$$

Stochastic equilibrium temperature modeling

- The identification of the parameters results in:

$$\begin{cases} A = \dfrac{\lambda}{c} \\ -AC = \dfrac{\Delta F}{c} \\ B + C = \Delta \mathcal{T}_s(0) \end{cases}$$

- The solutions are then $A = c^{-1}\lambda$,

$$C = -\frac{\Delta F}{Ac} = -\frac{\Delta F}{\lambda} = \Delta \mathcal{T}_s^{\star}$$

and:

$$B = \Delta \mathcal{T}_s(0) - C = \Delta \mathcal{T}_s(0) - \Delta \mathcal{T}_s^{\star}$$

- Finally, we conclude that:

$$\Delta \mathcal{T}_s(t) = \exp\left(-\frac{t}{\tau}\right)\left(\Delta \mathcal{T}_s(0) - \Delta \mathcal{T}_s^{\star}\right) + \Delta \mathcal{T}_s^{\star}$$

where:

$$\tau = -\frac{c}{\lambda}$$

Stochastic equilibrium temperature modeling

- $\Delta\mathcal{T}_s(t)$ is an exponential survival function with parameter τ^{-1}
- Using a specific heat capacity of $c = 4 \times 10^8\,\mathrm{J\,m^{-2}\,K^{-1}}$, we get:

$$\tau = -\frac{c}{\lambda} = -\frac{4 \times 10^8\,\mathrm{J\,m^{-2}\,K^{-1}}}{-1.33\,\mathrm{W\,m^{-2}\,K^{-1}}} = \frac{4 \times 10^8\,\mathrm{W\,m^{-2}\,K^{-1}\,s}}{1.33\,\mathrm{W\,m^{-2}\,K^{-1}}} = 3.0075 \times 10^8\,\mathrm{s}$$

- The relaxation time τ of the climate system is then equal to 3 480.92 days or 9.53 years
- Due to the exponential distribution, τ is also the mean lifetime
- Since we have:

$$\Delta\mathcal{T}_s(t) - \Delta\mathcal{T}_s^\star = \exp\left(-\frac{t}{\tau}\right)\left(\Delta\mathcal{T}_s(0) - \Delta\mathcal{T}_s^\star\right)$$

  the half-life $t_{1/2}$ is defined as the solution of the equation $\exp\left(-\frac{t_{1/2}}{\tau}\right) = \frac{1}{2}$ or $t_{1/2} = \tau \ln(2) = 6.61$ years
- The equilibrium is $\lim_{t\to\infty} \Delta\mathcal{T}_s(t) = \Delta\mathcal{T}_s^\star = 3.0075^\circ\mathrm{C}$.

Stochastic equilibrium temperature modeling

Figure 49: Surface temperature dynamics after a radiative forcing of $4\,\mathrm{W/m^2}$ ($\lambda = -1.33\,\mathrm{W\,m^{-2}\,K^{-1}}$)

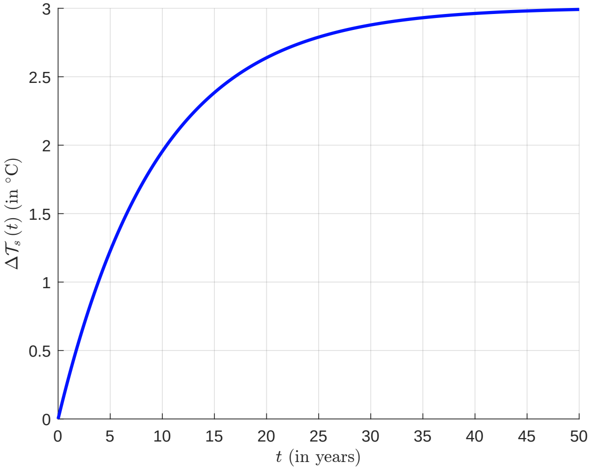

Stochastic equilibrium temperature modeling

Remark

The previous analysis assumes that the climate feedback parameter is certain. In fact, it is stochastic, which means that the equilibrium temperature and the temperature dynamics are stochastic

Stochastic equilibrium temperature modeling

- If $\tilde{\lambda} \sim \mathcal{N}\left(\mu_\lambda, \sigma_\lambda^2\right)$, the equilibrium temperature is equal to:

$$\Delta \widetilde{\mathcal{T}}_s^\star = -\frac{\Delta F}{\tilde{\lambda}} = \frac{1}{\xi}$$

where:

$$\xi = -\frac{\tilde{\lambda}}{\Delta F} \sim \mathcal{N}\left(\mu_\xi, \sigma_\xi^2\right) \equiv \mathcal{N}\left(-\frac{\mu_\lambda}{\Delta F}, \frac{\sigma_\lambda^2}{\Delta F^2}\right)$$

- We deduce that $\Delta \widetilde{\mathcal{T}}_s^\star$ follows a reciprocal normal distribution:

$$f(x) = \frac{1}{\sigma_\xi x^2 \sqrt{2\pi}} e^{-\frac{1}{2}\left(\frac{x^{-1}-\mu_\xi}{\sigma_\xi}\right)^2}$$

- Using the previous calibration of the climate feedback parameter $\tilde{\lambda} \sim \mathcal{N}\left(-1.30, 0.44^2\right)$, the distribution of $\Delta \widetilde{\mathcal{T}}_s^\star$ is right skewed and has an excess of kurtosis

Stochastic equilibrium temperature modeling

Figure 50: Probability density function of the equilibrium temperature ($\Delta F = 4\,\mathrm{W/m^2}$, $\mu_\lambda = -1.30\,\mathrm{W\,m^{-2}\,K^{-1}}$ and $\sigma_\lambda = 0.44\,\mathrm{W\,m^{-2}\,K^{-1}}$)

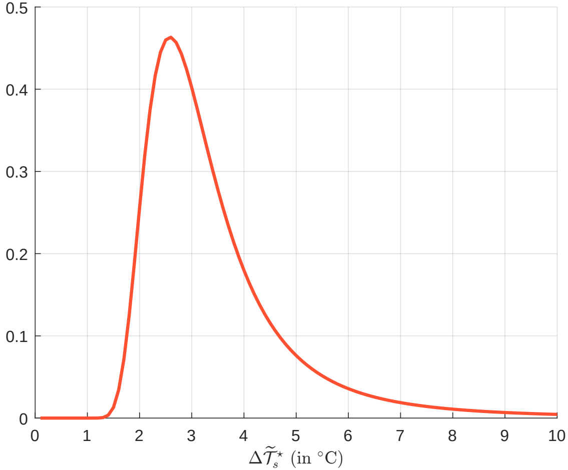

Stochastic equilibrium temperature modeling

- The cumulative distribution function and the exceedance probability are equal to:

Temperature θ	$2^\circ\mathrm{C}$	$3^\circ\mathrm{C}$	$4^\circ\mathrm{C}$	$5^\circ\mathrm{C}$	$7^\circ\mathrm{C}$	$10^\circ\mathrm{C}$
$\Pr\left\{\Delta\widetilde{\mathcal{T}}_s^\star \geq \theta\right\}$	94.26%	52.86%	24.61%	12.63%	4.73%	1.88%

- The probability of observing an equilibrium temperature greater than $4^\circ\mathrm{C}$ and $7^\circ\mathrm{C}$ is close to 25% and 5%

Stochastic equilibrium temperature modeling

- The mean lifetime follows a reciprocal normal distribution:

$$\tilde{\tau} = -\frac{c}{\tilde{\lambda}} \sim \mathcal{RN}\left(-\frac{\mu_\lambda}{c}, \frac{\sigma_\lambda^2}{c}\right)$$

Stochastic equilibrium temperature modeling

Figure 51: Probability density function of the relaxation time ($\mu_\lambda = -1.30\,\mathrm{W\,m^{-2}\,K^{-1}}$ and $\sigma_\lambda = 0.44\,\mathrm{W\,m^{-2}\,K^{-1}}$)

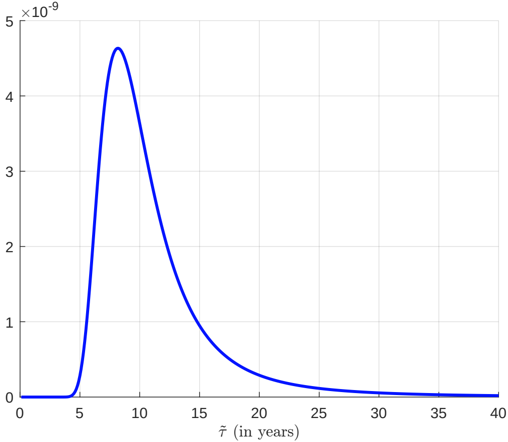

Stochastic equilibrium temperature modeling

Figure 52: Monte Carlo simulation of the surface temperature dynamics after a radiative forcing of $4\,\mathrm{W/m^2}$ ($\mu_\lambda = -1.30\,\mathrm{W\,m^{-2}\,K^{-1}}$ and $\sigma_\lambda = 0.44\,\mathrm{W\,m^{-2}\,K^{-1}}$)

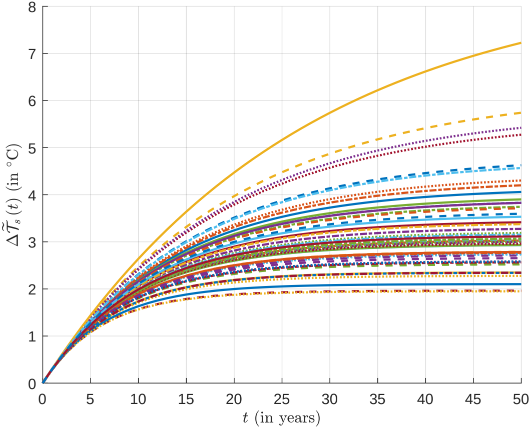

Equilibrium climate sensitivity estimation

- According to IPCC AR6, the total anthropogenic ERF[7] over the industrial era (1750-2019) is $2.72\,\mathrm{W/m^2}$
- The contribution of anthropogenic greenhouse gas emissions is $3.84\,\mathrm{W/m^2}$ and the combined effect of all radiative feedbacks (including Planck feedback) is estimated to be $-1.16\,\mathrm{W/m^2}$
- The best estimate of the ECS is $3^\circ\mathrm{C}$
- The likely range is $2.5^\circ\mathrm{C}$ to $4^\circ\mathrm{C}$ (with a probability of 66%), and the very likely range is $2^\circ\mathrm{C}$ to $5^\circ\mathrm{C}$ (with a probability of 90%)

[7] **Effective radiative forcing** (ERF) is a measure of the change in radiative flux at the top of the atmosphere and does not include the Planck feedback.

Equilibrium climate sensitivity estimation

Figure 53: Anthropogenic effective radiative forcing (ERF) from 1750 to 2019 by contributing forcing agents

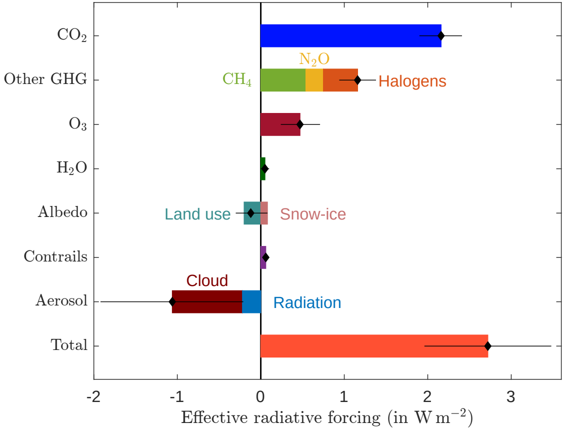

Source: IPCC (2021, Figure 7.6, Chapter 7, page 959).

Equilibrium climate sensitivity estimation

Table 12: Effective radiative forcing from 1750 to 2019

Forcing agent	1800	1850	1900	1950	2000	2010	2019
CO_2	0.070	0.140	0.346	0.648	1.561	1.854	2.156
CH_4	0.025	0.049	0.119	0.245	0.509	0.518	0.544
N_2O	0.004	0.007	0.032	0.069	0.157	0.181	0.208
Other GHG	0.000	0.000	0.000	0.010	0.375	0.392	0.408
O_3	0.015	0.030	0.081	0.167	0.399	0.443	0.474
H_2O (stratospheric)	0.002	0.005	0.011	0.022	0.047	0.048	0.050
Contrails	0.000	0.000	0.000	0.005	0.039	0.044	0.058
Aerosol	−0.018	−0.078	−0.346	−0.708	−1.221	−1.266	−1.058
Black carbon on snow	0.002	0.006	0.020	0.032	0.069	0.085	0.080
Land use	−0.011	−0.031	−0.084	−0.144	−0.194	−0.197	−0.200
Total (anthropogenic)	0.089	0.128	0.179	0.346	1.739	2.103	2.720
Volcanic	0.183	0.194	0.198	0.182	0.175	0.137	0.140
Solar	−0.043	0.008	−0.037	0.057	0.110	−0.008	−0.022
Total (natural)	0.140	0.202	0.160	0.239	0.285	0.129	0.118
Total	0.229	0.330	0.339	0.585	2.025	2.232	2.838

Source: IPCC (2021, Figure 7.6, Chapter 7, page 959).

Equilibrium climate sensitivity estimation

Figure 54: Contribution to effective radiative forcing (ERF) (a) and global mean surface air temperature (GSAT) change (b) from component emissions between 1750 to 2019 based on CMIP6 models

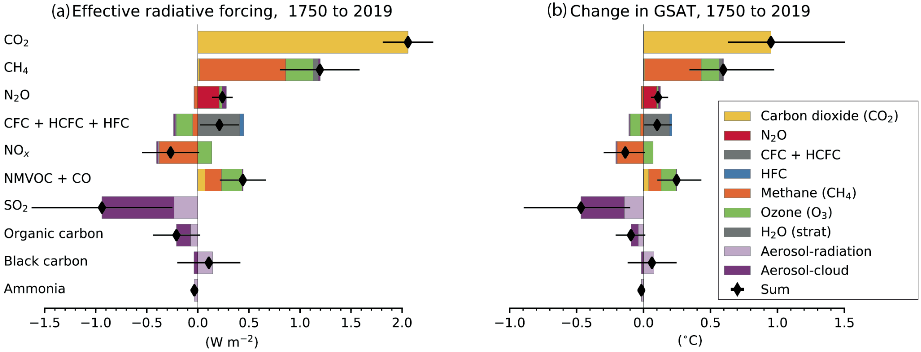

Source: IPCC (2021, Figure 6.12, Chapter 6, page 854).

Ratio distribution

Normal ratio distribution

- We assume that $X \sim \mathcal{N}\left(\mu_x, \sigma_x^2\right)$ and $Y \sim \mathcal{N}\left(\mu_y, \sigma_y^2\right)$
- $Z = X/Y \sim \mathcal{NRD}\left(\mu_x, \sigma_x^2, \mu_y, \sigma_y^2\right)$
- The CDF of Z is:

$$\mathbf{F}_z\left(z\right) = \Phi_2\left(-\frac{\mu_y z - \mu_x}{\sigma_x \sigma_y a\left(z\right)}, -\frac{\mu_y}{\sigma_y}, \rho_z\right) + \Phi_2\left(\frac{\mu_y z - \mu_x}{\sigma_x \sigma_y a\left(z\right)}, \frac{\mu_y}{\sigma_y}, \rho_z\right)$$

- The PDF of Z is:

$$f_z\left(z\right) = \frac{b\left(z\right)}{\sigma_x \sigma_y \sqrt{2\pi} a^3\left(z\right)}\left(2\Phi\left(\frac{b\left(z\right)}{a\left(z\right)}\right) - 1\right)\exp\left(\frac{b^2\left(z\right) - ca^2\left(z\right)}{2a^2\left(z\right)}\right) + \frac{1}{\sigma_x \sigma_y a^2\left(z\right)\pi}\exp\left(-\frac{c}{2}\right)$$

- $a\left(z\right) = \sqrt{\frac{1}{\sigma_x^2}z^2 + \frac{1}{\sigma_y^2}}$, $b\left(z\right) = \frac{\mu_x}{\sigma_x^2}z + \frac{\mu_y}{\sigma_y^2}$, $c = \frac{\mu_x^2}{\sigma_x^2} + \frac{\mu_y^2}{\sigma_y^2}$ and $\rho_z = \frac{z}{\sigma_x a\left(z\right)}$

Equilibrium climate sensitivity estimation

We now have all the information we need to calculate the equilibrium climate sensitivity

Equilibrium climate sensitivity estimation

- Using the parameters from Sherwood *et al.* (2020) $\lambda \sim \mathcal{N}\left(-1.30, 0.44^2\right)$ and $\Delta F_{2\times\mathrm{CO}_2} \sim \mathcal{N}\left(4.00, 0.30^2\right)$, we get:

$$\begin{aligned} \mathrm{ECS} &= -\frac{\Delta F_{2\times\mathrm{CO}_2}}{\lambda} \\ &= -\frac{\mathcal{N}\left(4.00, 0.30^2\right)}{\mathcal{N}\left(-1.30, 0.44^2\right)} \\ &= \mathcal{NRD}\left(-4.00, 0.30^2, -1.30, 0.44^2\right) \end{aligned}$$

  where $\mathcal{NRD}$ is the normal ratio distribution

- The exceedance probability is equal to:

Temperature θ	$2^\circ\mathrm{C}$	$3^\circ\mathrm{C}$	$4^\circ\mathrm{C}$	$5^\circ\mathrm{C}$	$7^\circ\mathrm{C}$	$10^\circ\mathrm{C}$
$\Pr\{\mathrm{ECS} \geq \theta\}$	93.24%	52.79%	24.92%	12.85%	4.81%	1.91%

- We have a probability about 25% to observe a global warming greater than $4^\circ\mathrm{C}$

Equilibrium climate sensitivity estimation

Figure 55: Probability density function of the equilibrium climate sensitivity ($\Delta F = +4.00\,\mathrm{W/m^2}$, $\sigma(\Delta F) = 0.30\,\mathrm{W/m^2}$, $\mu_\lambda = -1.30\,\mathrm{W\,m^{-2}\,K^{-1}}$ and $\sigma_\lambda = 0.44\,\mathrm{W\,m^{-2}\,K^{-1}}$)

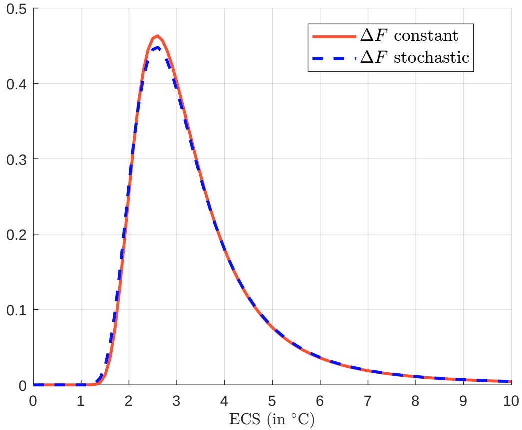

An example of unstable equilibrium

- In the Budyko model, we have at equilibrium:

$$\mathcal{E} = \frac{1}{4}\left(1 - \alpha_p\left(\mathcal{T}_s\right)\right) S_0 - \left(\frac{2-\varepsilon}{2}\right)\sigma \mathcal{T}_s^4 = 0$$

where:

$$\alpha_p\left(\mathcal{T}_s\right) = \begin{cases} \alpha_{\mathrm{cold}} & \text{if } \mathcal{T}_s \leq \mathcal{T}_{\mathrm{cold}} \\ \alpha_{\mathrm{warm}} + \left(\alpha_{\mathrm{cold}} - \alpha_{\mathrm{warm}}\right)\left(\dfrac{\mathcal{T}_{\mathrm{warm}} - \mathcal{T}_s}{\mathcal{T}_{\mathrm{warm}} - \mathcal{T}_{\mathrm{cold}}}\right)^{\eta} & \text{if } \mathcal{T}_{\mathrm{cold}} \leq \mathcal{T}_s \leq \mathcal{T}_{\mathrm{warm}} \\ \alpha_{\mathrm{warm}} & \text{if } \mathcal{T}_s \geq \mathcal{T}_{\mathrm{warm}} \end{cases}$$

- The two forcing functions are

$$\begin{cases} F_{\mathrm{solar}}\left(\mathcal{T}_s\right) = \dfrac{1}{4}\left(1 - \alpha_p\left(\left(\mathcal{T}_s\right)\right)\right) S_0 \\ F_{\mathrm{blackbody}}\left(\mathcal{T}_s\right) = \left(\dfrac{2-\varepsilon}{2}\right)\sigma \mathcal{T}_s^4 \end{cases}$$

An example of unstable equilibrium

Figure 56: Equilibrium states of the Budyko ice-albedo model

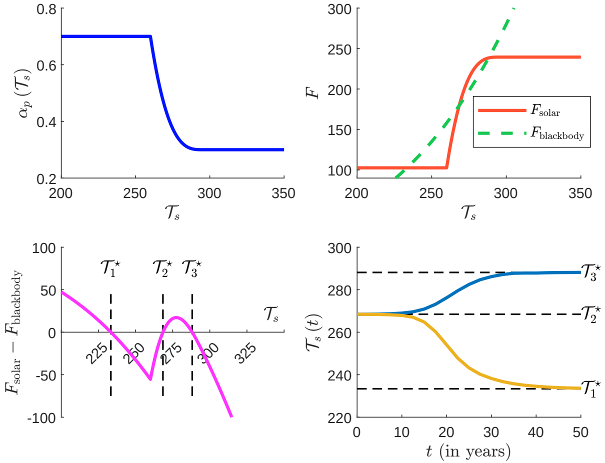

An example of unstable equilibrium

There are three equilibrium states:

1. $\mathcal{T}_1^\star = 233.38\,\mathrm{K}$
2. $\mathcal{T}_2^\star = 268.43\,\mathrm{K}$
3. $\mathcal{T}_3^\star = 288.13\,\mathrm{K}$

An example of unstable equilibrium

The total feedback is equal to:

$$\lambda\left(\mathcal{T}_s\right) = \lambda_0\left(\mathcal{T}_s\right) + \lambda_{\alpha_p}\left(\mathcal{T}_s\right)$$

where:

$$\lambda_0\left(\mathcal{T}_s\right) = -4\left(\frac{2-\varepsilon}{2}\right)\sigma\mathcal{T}_s^3$$

and:

$$\lambda_{\alpha_p}\left(\mathcal{T}_s\right) = \frac{1}{4}\eta S_0\left(\alpha_{\mathrm{cold}} - \alpha_{\mathrm{warm}}\right)\frac{\left(\mathcal{T}_{\mathrm{warm}} - \mathcal{T}_s\right)^{\eta-1}}{\left(\mathcal{T}_{\mathrm{warm}} - \mathcal{T}_{\mathrm{cold}}\right)^{\eta}}\cdot\mathbb{1}\left\{\mathcal{T}_{\mathrm{cold}} \leq \mathcal{T}_s \leq \mathcal{T}_{\mathrm{warm}}\right\}$$

State	Temperature		$\lambda_0\left(\mathcal{T}_s\right)$	$\lambda_{\alpha_p}\left(\mathcal{T}_s\right)$	$\lambda\left(\mathcal{T}_s\right)$
$\mathcal{T}_1^\star$	$233.38\,\mathrm{K}$	$-39.77^\circ\mathrm{C}$	-1.76	0.00	-1.76
$\mathcal{T}_2^\star$	$268.43\,\mathrm{K}$	$-4.72^\circ\mathrm{C}$	-2.68	6.75	$+4.08$
$\mathcal{T}_3^\star$	$288.13\,\mathrm{K}$	$14.98^\circ\mathrm{C}$	-3.31	0.45	-2.86

An example of unstable equilibrium

- $\mathcal{T}_1^\star$ and $\mathcal{T}_3^\star$ are two stable equilibria because λ is negative, but $\mathcal{T}_2^\star$ is an unstable equilibrium
- To illustrate this instability, we consider the dynamics of the temperature:

$$c\frac{\mathrm{d}\mathcal{T}_s}{\mathrm{d}t} = F_{\text{solar}}\left(\mathcal{T}_s\right) - F_{\text{blackbody}}\left(\mathcal{T}_s\right) + \Delta F$$

  where $c = 4 \times 10^8\,\mathrm{J\,m^{-2}\,K^{-1}}$ is the heat capacity and ΔF is the perturbation
- The fourth panel shows a small perturbation $\Delta F = \pm 0.1\,\mathrm{W/m^2}$

An example of unstable equilibrium

Figure 57: Equilibrium states of the Budyko ice-albedo model

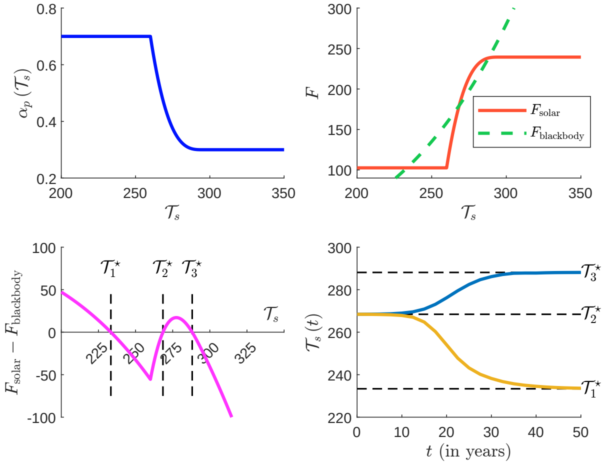

Tipping point definition

- The concept of a tipping point emerged from stability analysis and bifurcation
- The term was popularized in 2000 by Malcolm Gladwell in his book "***The Tipping Point: How Little Things Can Make a Big Difference***", which explored the concept in sociological change
- In climate change, it was popularized in the late 2000s by Lenton *et al.* (2008)
- In common parlance, a tipping point is a change

Tipping point definition

"The term tipping point commonly refers to a critical threshold at which a tiny perturbation can qualitatively alter the state or development of a system." (Lenton et al., 2008, page 1786).

"A climate tipping point occurs when a small change in forcing triggers a strongly nonlinear response in the internal dynamics of part of the climate system, qualitatively changing its future state." (Lenton et al., 2011, page 201).

"Tipping points refer to critical thresholds in a system that, when exceeded, can lead to a significant change in the state of the system, often with an understanding that the change is irreversible." (IPCC, 2018, page 262).

A tipping point is "a hypothesized critical threshold when global or regional climate changes from one stable state to another stable state. The tipping point event may be irreversible." (IPCC, 2021, page 1463).

Bifurcation theory

Figure 58: Stable equilibria

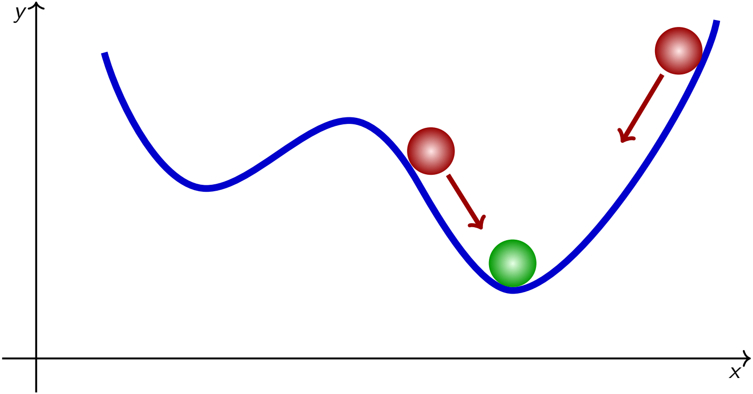

Bifurcation theory

Figure 59: Unstable equilibrium

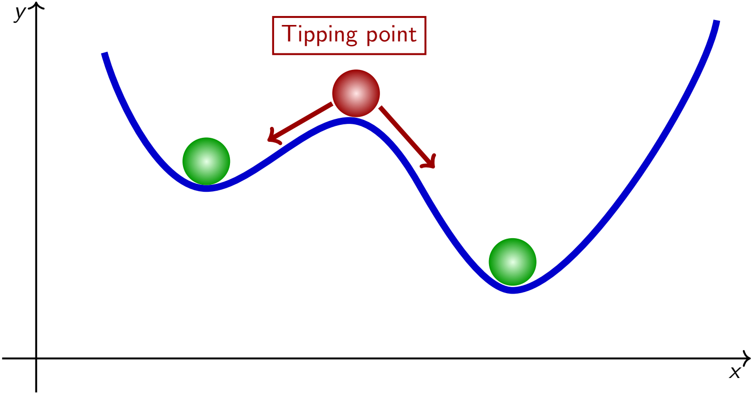

Bifurcation theory

Figure 60: Irreversible tipping point

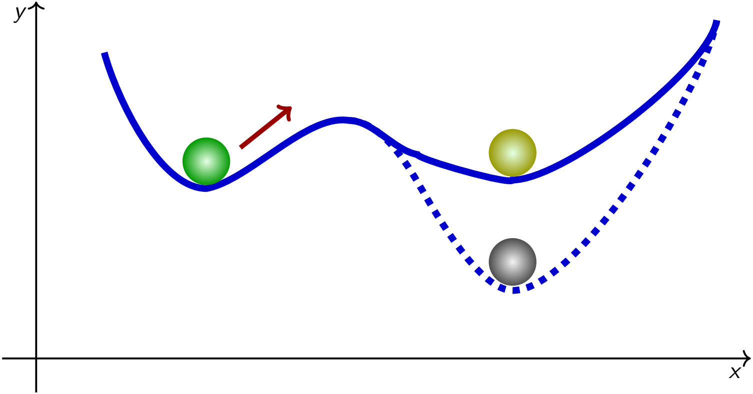

Bifurcation theory

- We consider the dynamical system of the form:

$$\frac{\mathrm{d}x}{\mathrm{d}t} = f(x, \mu)$$

  where μ is the parameter set
- If $f(x, \mu) > 0$, then x increases with time, while if $f(x, \mu) < 0$, then x decreases with time
- A fixed point $x^\star$ is then a value of x such that the system does not change with time, *i.e.* $f(x^\star, \mu) = 0$
- Let $x = x^\star + \Delta x$ where Δx is small. We have:

$$\begin{aligned}\frac{\mathrm{d}x}{\mathrm{d}t} &= f(x^\star + \Delta x, \mu) \\ &= f(x^\star, \mu) + \frac{\partial f(x^\star, \mu)}{\partial x}\Delta x + O\left(\Delta x^2\right) \\ &= f(x^\star, \mu) + \lambda \Delta x + \mathcal{O}\left(\Delta x^2\right)\end{aligned}$$

  where λ is the feedback of the system

Bifurcation theory

- Since we have:

$$\frac{\mathrm{d}x}{\mathrm{d}t} = \frac{\mathrm{d}\left(x^{\star} + \Delta x\right)}{\mathrm{d}t} = \frac{\mathrm{d}\Delta x}{\mathrm{d}t}$$

  and:

$$f\left(x^{\star} + \Delta x, \mu\right) \approx f\left(x^{\star}, \mu\right) + \lambda \Delta x = \lambda \Delta x$$

- We deduce that:

$$\frac{\mathrm{d}\Delta x}{\mathrm{d}t} = \lambda \Delta x$$

- If $\lambda > 0$, then any small perturbation of the fixed point grows exponentially (**the fixed point is unstable**)
- If $\lambda < 0$, then any small perturbation of the fixed point decays exponentially (**the fixed point is stable**)
- The relaxation timescale is equal to:

$$\tau = \frac{1}{\left|\partial_x f\left(x^{\star}, \mu\right)\right|}$$

Bifurcation theory

Example #1

We consider the dynamical system $\frac{\mathrm{d}x}{\mathrm{d}t} = x^2 + \mu$

Bifurcation theory

- We have $\partial_x f(x, \mu) = 2x$
- The fixed points are solutions of the equation $x^2 = -\mu$
- If $\mu > 0$, there are no fixed points
- If $\mu = 0$, the fixed point is $x^\star = 0$ and is not stable
- If $\mu < 0$, there are two fixed points. $x_1^\star = -\sqrt{-\mu}$ is stable while $x_2^\star = \sqrt{-\mu}$ is unstable

Bifurcation theory

- The stability analysis evaluates the behavior of $f(x^{\star}+\varepsilon,\mu)$ and checks if the point $x^{\star}+\Delta x$ converges to the point $x^{\star}$
- We can consider a second approach to stability where we evaluate the behavior of $f(x^{\star},\mu+\varepsilon)$, *i.e.* we apply the perturbation not directly to x but to the control parameter
- We say that the value $\mu^{\star}$ is a bifurcation value if $f(x,\mu^{\star})$ is not structurally stable

Bifurcation theory

- In the previous example, the dynamical system exhibits a bifurcation that occurs at $\mu = 0$
- This type of bifurcation is called a saddle-node or fold bifurcation, because fixed points are created or destroyed

Bifurcation theory

Figure 61: Bifurcation diagram

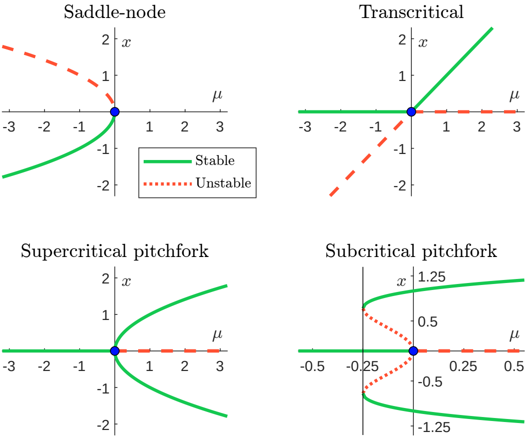

Bifurcation theory

- A transcritical bifurcation occurs when fixed points exchange stability for a critical value of μ
- For example, the system $\dfrac{\mathrm{d}x(t)}{\mathrm{d}t} = \mu x - x^2$ has a transcritical bifurcation at $\mu = 0$

Bifurcation theory

Figure 62: Bifurcation diagram

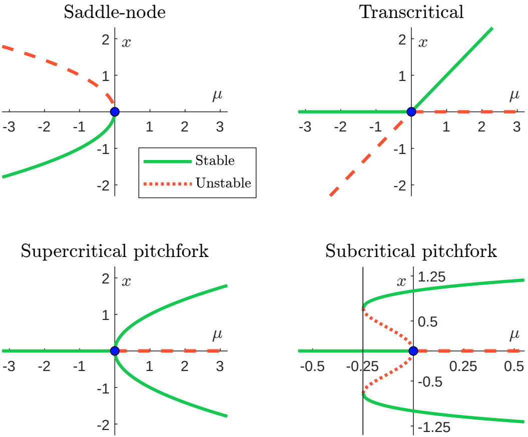

Bifurcation theory

- A pitchfork bifurcation occurs when the system is unchanged and exhibits symmetry when $x = -x$. There are two forms of pitchfork bifurcation:
  1. In a supercritical pitchfork bifurcation, a stable fixed point becomes unstable at a critical value of μ. A canonical example is:

  $$\frac{\mathrm{d}x}{\mathrm{d}t} = \mu x - x^3$$

  2. In a subcritical pitchfork bifurcation, an unstable fixed point becomes stable at a critical value of μ. A canonical example is:

  $$\frac{\mathrm{d}x}{\mathrm{d}t} = \mu x + x^3 - x^5$$

Bifurcation theory

Figure 63: Bifurcation diagram

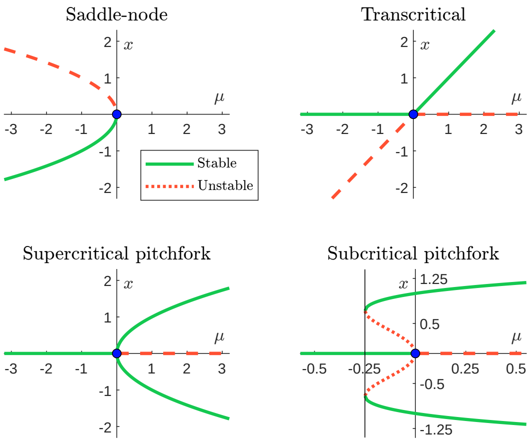

Hysteresis

Definition

In bifurcation theory, hysteresis refers to a phenomenon where the behavior of the system depends on the history of its past states

Hysteresis

- Consider the previous subcritical pitchfork bifurcation and suppose the system is at equilibrium $x^\star = 0$
- If we increase μ, the system jumps to one of the stable branches
- If we decrease μ, the system does not return to its past equilibrium, but stays on the stable branch
- However, if we decrease μ even more, the system jumps to its past equilibrium $x^\star = 0$ when μ reaches $\mu^\star = -0.25$
- The path of the system has formed a **hysteresis loop**

Bifurcation theory

Figure 64: Bifurcation diagram

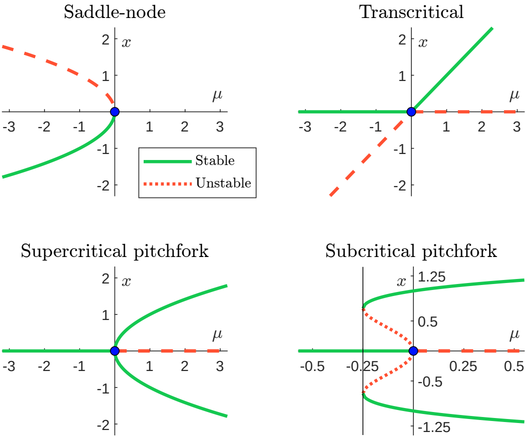

Chaos theory

Rössler model

- The Rössler model is a system of ordinary differential equations that exhibits chaotic dynamics:

$$\left\{ \begin{array}{l} \dfrac{\mathrm{d}x(t)}{\mathrm{d}t} = -\left(y(t) + z(t)\right) \\ \dfrac{\mathrm{d}y(t)}{\mathrm{d}t} = x(t) + ay(t) \\ \dfrac{\mathrm{d}z(t)}{\mathrm{d}t} = b + x(t)z(t) - cz(t) \end{array} \right.$$

  where a, b and c are three parameters that control the behavior of the system
- The Rössler attractor is a three-dimensional surface described by $(x(t), y(t), z(t))$
- The attractor is very sensitive to the initial conditions $(x(0), y(0), z(0))$ and the set of parameters (a, b, c)

Chaos theory

Figure 65: Rössler attractor

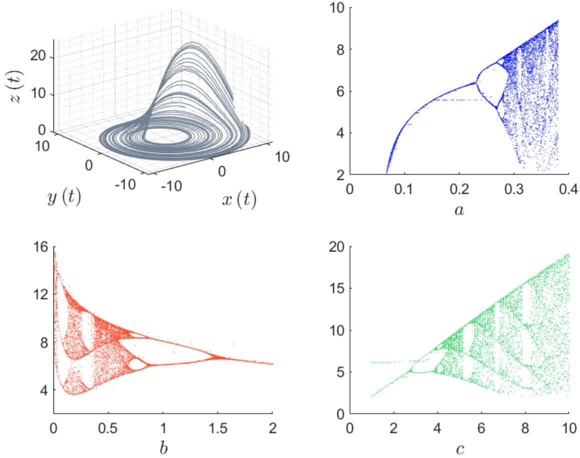

Application to the Budyko ice-albedo model

- We use the default values $S_0 = 1\,368\,\mathrm{W/m^2}$, $\varepsilon = 78\%$, $\eta = 3$, $\alpha_{\mathrm{cold}} = 0.7$, $\mathcal{T}_{\mathrm{cold}} = 260\,\mathrm{K}$, $\alpha_{\mathrm{warm}} = 0.3$ and $\mathcal{T}_{\mathrm{warm}} = 295\,\mathrm{K}$
- We have three fixed points: $\mathcal{T}_1^\star = 233.38\,\mathrm{K}$, $\mathcal{T}_2^\star = 268.43\,\mathrm{K}$, and $\mathcal{T}_3^\star = 288.13\,\mathrm{K}$
- $\mathcal{T}_1^\star$ and $\mathcal{T}_3^\star$ are stable
- $\mathcal{T}_3^\star$ is unstable

Application to the Budyko ice-albedo model

- To perform the bifurcation analysis of the Budyko ice-albedo model, we consider the range $\mathcal{T}_s \in [200\,\mathrm{K}, 300\,\mathrm{K}]$ and divide the range into ten intervals
- Using the bisection algorithm, we solve the equation for each interval of $\mathcal{T}_s$ and each value of the parameter of interest:

$$\frac{1}{4}\left(1 - \alpha_p\left(\left(\mathcal{T}_s\right)\right)\right) S_0 - \left(\frac{2-\varepsilon}{2}\right)\sigma \mathcal{T}_s^4 = 0$$

- We collect all fixed points $\{\mathcal{T}_1^\star, \mathcal{T}_2^\star, \ldots\}$
- For each fixed point we calculate the feedback:

$$\begin{aligned}\lambda\left(\mathcal{T}_s\right) &= \frac{1}{4}\eta S_0\left(\alpha_{\mathrm{cold}} - \alpha_{\mathrm{warm}}\right)\frac{\left(\mathcal{T}_{\mathrm{warm}} - \mathcal{T}_s\right)^{\eta-1}}{\left(\mathcal{T}_{\mathrm{warm}} - \mathcal{T}_{\mathrm{cold}}\right)^{\eta}}\cdot \\ & \mathbb{1}\left\{\mathcal{T}_{\mathrm{cold}} \leq \mathcal{T}_s \leq \mathcal{T}_{\mathrm{warm}}\right\} - 4\left(\frac{2-\varepsilon}{2}\right)\sigma\mathcal{T}_s^3\end{aligned}$$

Application to the Budyko ice-albedo model

Figure 66: Bifurcation of the Budyko ice-albedo model

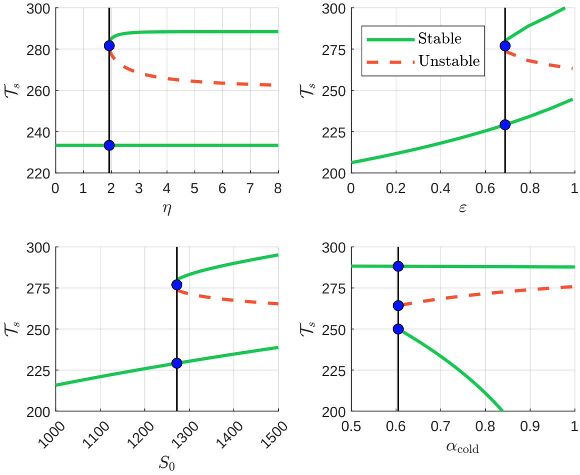

Application to the Budyko ice-albedo model

The relaxation timescale is equal to:

$$\tau = \frac{c}{\left|\lambda\left(\mathcal{T}_s\right)\right|}$$

where $c = 4 \times 10^8 \, \mathrm{J\,m^{-2}\,K^{-1}}$ is the heat capacity

Application to the Budyko ice-albedo model

Figure 67: Relaxation timescale of the Budyko ice-albedo model (in years)

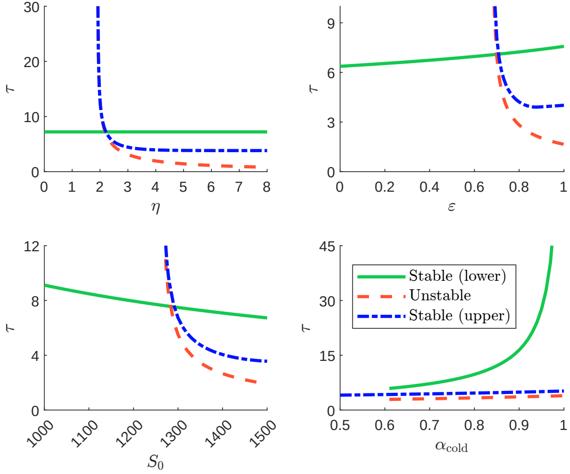

Bifurcation theory

Figure 68: Bifurcation and overshooting tipping points

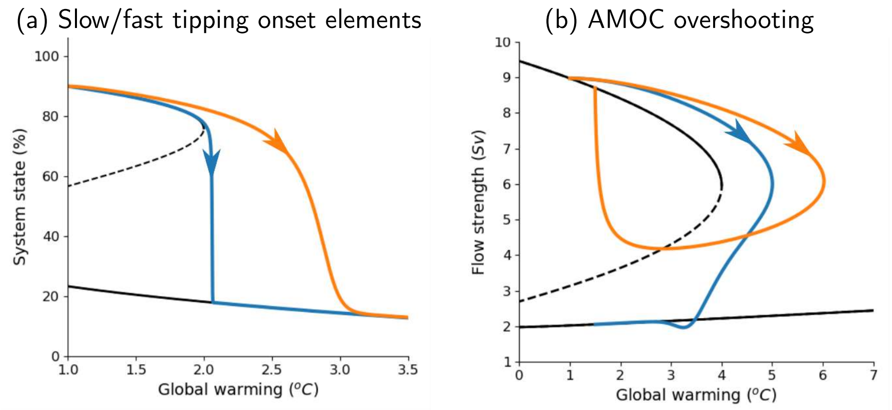

Source: Ritchie *et al.* (2021, Figures 1c & 3c, pages 518 & 520).

Climate tipping elements

Figure 69: Geographical distribution of global and regional tipping elements

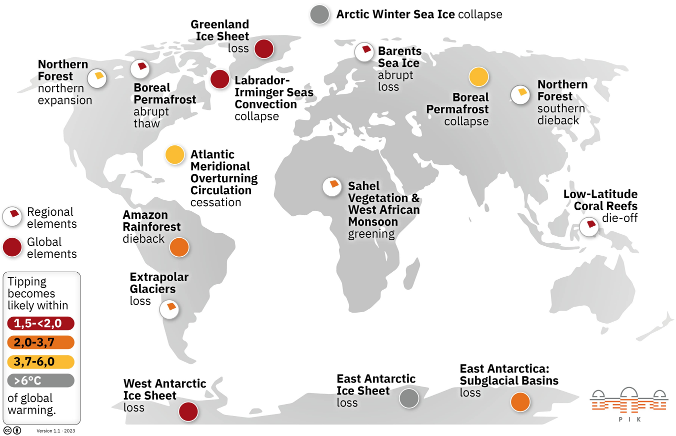

Source: Armstrong McKay *et al.* (2022).

Climate tipping elements

Table 13: Threshold, timescale, and impact estimates for the global and regional tipping elements

Category	#	Climate tipping element	Tipping point	Threshold		Timescale		Maximum impact	
Global	1	Greenland ice sheet	collapse	1.5°C	(0.8-3.0)	10 kyr	(1-15)	0.13°C	(0.5-3.0)
	2	West Antarctic ice sheet	collapse	1.5°C	(1.0-3.0)	2 kyr	(0.5-13)	0.05°C	(1.0)
	3	Labrador-Irminger seas	collapse	1.8°C	(1.1-3.8)	10 yr	(5-50)	−0.50°C	(-3.0)
	4	East Antarctic subglacial basins	collapse	3.0°C	(2.0-6.0)	2 kyr	(0.5-10)	0.05°C	
	5	Amazon rainforest	dieback	3.5°C	(2.0-6.0)	100 yr	(50-200)	0.20°C	(0.4-2.0)
	6	Boreal permafrost	collapse	4.0°C	(3.0-6.0)	50 yr	(10-300)	0.40°C	
	7	AMOC	collapse	4.0°C	(1.4-8.0)	50 yr	(15-300)	−0.50°C	(-4/-10)
	8	Arctic winter sea ice	collapse	6.3°C	(4.5-8.7)	20 yr	(10-100)	0.60°C	(0.6-1.2)
	9	East Antarctic ice sheet	collapse	7.5°C	(5.0-10.0)	> 10 kyr		0.60°C	(2.0)
Regional	10	Low-latitude coral reefs	die-off	1.5°C	(1.0-2.0)	10 yr			
	11	Boreal permafrost	abrupt thaw	1.5°C	(1.0-2.3)	200 yr	(100-300)	0.04°C	
	12	Barents sea ice	abrupt loss	1.6°C	(1.5-1.7)	25 yr			
	13	Mountain glaciers	loss	2.0°C	(1.5-3.0)	200 yr	(50-1000)	0.08°C	
	14	Sahel and West African monsoon	greening	2.8°C	(2.0-3.5)	50 yr	(10-500)		
	15	Boreal forest (southern)	die-off	4.0°C	(1.4-5.0)	100 yr	(50+)	−0.18°C	(-0.5/-2)
	16	Boreal forest (northern)	expansion	4.0°C	(1.5-7.2)	100 yr	(40+)	0.14°C	(0.5-1.0)

Source: Armstrong McKay *et al.* (2022, Table 1, page 3).

Climate tipping elements

1. Greenland ice sheet

The Greenland ice sheet is the second largest ice sheet in the world. It covers 80% of the surface of Greenland. Its melting would increase sea level rise, possibly up to 7.4 meters, accelerate ocean acidification, and have a potentially positive feedback effect on climate change.

Climate tipping elements

2. West Antarctic ice sheet

The West Antarctic ice sheet is a large ice sheet in Antarctica. It sits on a bedrock that is mostly below sea level and has formed a deep subglacial basin due to the weight of the ice sheet, which can be up to 4 kilometers thick in places. Its collapse could raise global sea levels, possibly up to 3 meters.

Climate tipping elements

3. Labrador-Irminger seas

The Labrador and Irminger seas are located in the subpolar North Atlantic, between Canada, Greenland and Iceland. These seas are characterized by cold and salty waters that generate deep convection. This deep convection and the regulation of ocean salinity influence the circulation of the Atlantic meridional overturning circulation (AMOC). The collapse of the deep convection system in the Labrador and Irminger seas would affect the overall circulation in the North Subpolar Gyre.

Climate tipping elements

4. East Antarctic subglacial basins

East Antarctic subglacial basins are large, ice-filled depressions in the bedrock adjacent to the East Antarctic ice sheet. They also serve as reservoirs for meltwater. Certain subglacial basins, such as Wilkes, Aurora, and Recovery, are more susceptible to a situation called marine ice sheet instability (MISI). As the ice shelf at the edge of the ice sheet retreats, warm ocean water can flow into the deeper basin, further destabilizing the ice shelf. This process can create a self-perpetuating cycle of ice melt and ice shelf retreat.

Climate tipping elements

5. Amazon rainforest

The Amazon rainforest, also known as the Amazon jungle or Amazonia, is the largest rainforest in the world. It spans nine countries: Brazil, Peru, Colombia, Ecuador, Bolivia, Venezuela, Guyana, Suriname, and French Guiana. It contains the largest and most biodiverse area of tropical rainforest in the world. The Amazon rainforest acts as a massive carbon sink, absorbing and storing vast amounts of carbon dioxide through the process of photosynthesis. If the forest were to be subject to widespread deforestation or degradation, the stored carbon could be released back into the atmosphere, contributing to increased greenhouse gas concentrations. The Amazon also plays a critical role in the Earth's water cycle, influencing regional and global weather patterns. Its dense vegetation effectively captures rainwater and slowly releases it into streams and rivers, helping to maintain stable water levels, prevent flooding, and provide a steady source of fresh water.

Climate tipping elements

6. Boreal permafrost

Boreal permafrost is a permanently frozen layer of soil and rock that underlies much of the world's boreal forest. It is found in Siberia, Alaska, Northern Canada, and the Tibetan Plateau. Permafrost forms when the soil temperature remains below $0^{\circ}\mathrm{C}$ for at least two consecutive years. Boreal permafrost contains large amounts of organic carbon stored in the form of dead plant material that could not decompose due to the cold temperatures. It is also one of the largest reservoirs of methane. Rising temperatures may cause the boreal permafrost to thaw, releasing large amounts of carbon and methane into the atmosphere.

Climate tipping elements

7. AMOC

The Atlantic meridional overturning circulation (AMOC) is a large, complex system of ocean currents that transports warm water from the tropics to the North Atlantic and cold water from the North Atlantic to the subtropics. It is also known as the Gulf Stream system. A weakening of the AMOC could have complex and regionally specific effects on temperatures. On a global scale, it could result in less warm water reaching higher latitudes, leading to cooler sea surface temperatures in the North Atlantic and warmer temperatures in the Southern Hemisphere.

Climate tipping elements

8. Arctic winter sea ice

Arctic winter sea ice is the maximum extent of sea ice that forms in the Arctic Ocean during the winter months. It helps to regulate global temperatures by reflecting sunlight back into space. This albedo reflection helps to cool the Arctic. As sea ice melts, more sunlight is absorbed by the ocean, causing a further warming trend[a]. However, the impact of the albedo effect remains controversial.

[a] Moreover, the warming Arctic has the potential to release methane from permafrost.

Climate tipping elements

9. East Antarctic ice sheet

The East Antarctic ice sheet is the largest and thickest ice sheet on Earth. A complete collapse would raise the global sea levels by 50 meters. However, the East Antarctic ice sheet is generally considered to be more stable than the West Antarctic ice sheet, due to its higher elevation and more remote location.

Climate tipping elements

10. Low-latitude coral reefs

Low-latitude coral reefs occur in the Atlantic, Indian, and Pacific Oceans, most notably in the Philippines, Indonesia, and Australia. They require warm, sunny weather and unpolluted water. Therefore, coral reefs can be affected by climate change, although their impact on climate change is more limited.

Climate tipping elements

11. Boreal permafrost

We have already seen that the boreal permafrost is a global tipping element, but it is also a regional tipping element. In fact, an abrupt thaw of the boreal permafrost would have devastating consequences for the region, affecting infrastructure (roads, buildings, transportation), the environment (flooding, forests, vegetation), and living conditions and health.

Climate tipping elements

12. Barents sea ice

Barents sea ice is found in the Barents sea, an arm of the Arctic Ocean between Norway and Russia. The sea ice forms during the winter months and melts during the summer months. This regional tipping element is strongly related to two global tipping elements: Labrador-Irminger seas and AMOC.

Climate tipping elements

13. Mountain glaciers

Mountain glaciers are large masses of ice that form on mountains at high altitudes. They are formed from compacted snow that has accumulated over many years. The melting of mountain glaciers would have a major regional impact on human life.

Climate tipping elements

14. Sahel and West African monsoon

The West African monsoon is a seasonal wind pattern that affects the Sahel, bringing moisture from the Atlantic Ocean during the rainy season and drying out the region during the dry season. It is responsible for the region's agriculture and supports the livelihoods of millions of people. Changes in rainfall can affect vegetation, agriculture and people.

Climate tipping elements

15. Boreal forest (southern)

The boreal forest, also known as the taiga, is a biome that surrounds the Arctic region. Countries with significant areas of boreal forest include Canada, Russia, Sweden, Norway and Finland. The southern edge of the boreal forest is the boundary between the boreal forest and temperate forests or grasslands. The risk could be an abrupt die-off.

Climate tipping elements

16. Boreal forest (northern)

The northern edge of the boreal forest is typically found at higher latitudes, closer to the Arctic Circle. The change could be an abrupt expansion into a tundra forest characterised by treeless landscapes and permafrost.

Cascading tipping points and climate domino effects

Figure 70: Double fold bifurcation

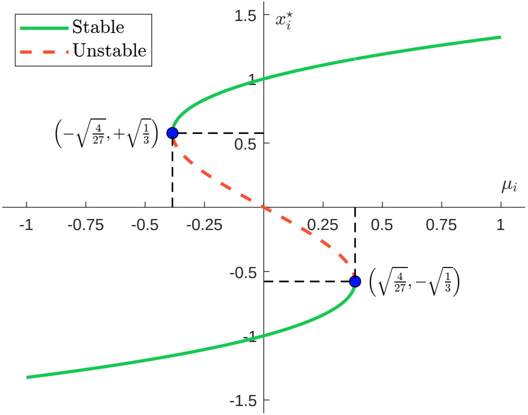

Source: Klose *et al.* (2020, Figure 1, page 3).

Cascading tipping points and climate domino effects

Figure 71: Convergence to the equilibrium

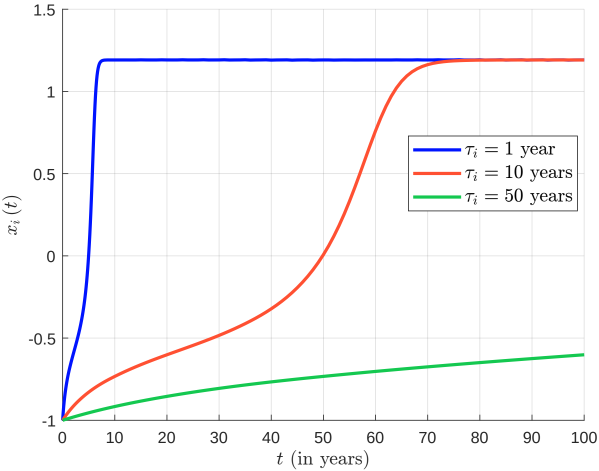

Cascading tipping points and climate domino effects

Figure 72: Master-slave bifurcation

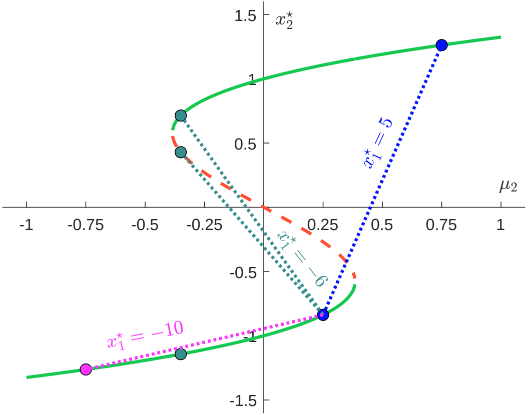

Source: Klose *et al.* (2020, Figure 2, page 6).

Cascading tipping points and climate domino effects

Figure 73: Equilibria of the slave subsystem

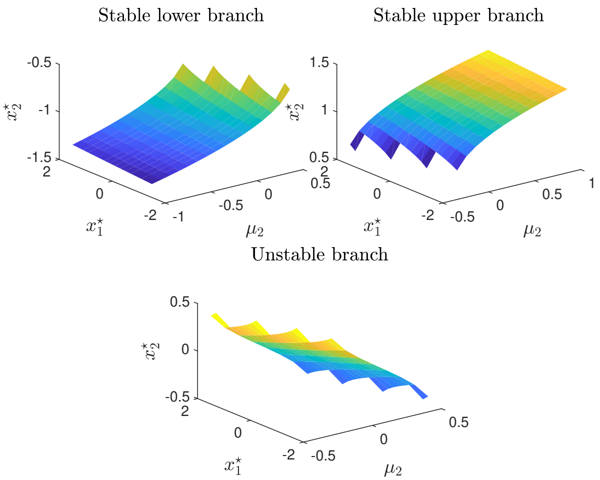

Cascading tipping points and climate domino effects

Figure 74: Interactions between climate tipping elements and their roles in tipping cascades

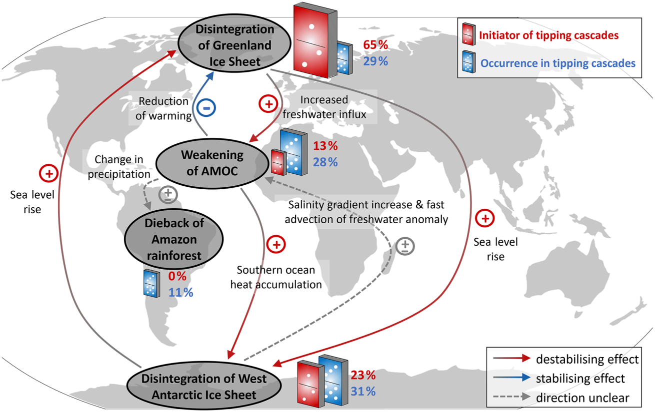

Source: Wunderling *et al.* (2021, Figure 1, page 603).